THE JOURNAL OF IMMUNOLOGY

Calcium Signaling via Orai1 Is Essential for Induction of the Nuclear Orphan Receptor Pathway To Drive Th17 Differentiation

Kyun-Do Kim, Sonal Srikanth, Yossan-Var Tan, Ma-Khin Yee, Marcus Jew, Robert Damoiseaux, Michael E. Jung, Saki Shimizu, Dong Sung An, Bernard Ribalet, James A. Waschek and Yousang Gwack

J Immunol 2014; 192:110-122; Prepublished online 4 December 2013;
doi: 10.4049/jimmunol.1302586
http://www.jimmunol.org/content/192/1/110

The Journal of Immunology is published twice each month by
The American Association of Immunologists, Inc.,
9650 Rockville Pike, Bethesda, MD 20814-3994.

Print ISSN: 0022-1767 Online ISSN: 1550-6606.

Calcium Signaling via Orai1 Is Essential for Induction of the Nuclear Orphan Receptor Pathway To Drive Th17 Differentiation

Kyun-Do Kim,*[,1] Sonal Srikanth,*[,1] Yossan-Var Tan,[†] Ma-Khin Yee,* Marcus Jew,* Robert Damoiseaux,[‡] Michael E. Jung,[§] Saki Shimizu,[¶,‖] Dong Sung An,[¶,‖,#] Bernard Ribalet,* James A. Waschek,[†] and Yousang Gwack*

Orai1 is the pore subunit of Ca^{2+} release–activated Ca^{2+} (CRAC) channels that stimulate downstream signaling pathways crucial for T cell activation. CRAC channels are an attractive therapeutic target for alleviation of autoimmune diseases. Using high-throughput chemical library screening targeting Orai1, we identified a novel class of small molecules that inhibit CRAC channel activity. One of these molecules, compound 5D, inhibited CRAC channel activity by blocking ion permeation. When included during differentiation, Th17 cells showed higher sensitivity to compound 5D than Th1 and Th2 cells. The selectivity was attributable to high dependence of promoters of retinoic-acid-receptor-related orphan receptors on the Ca^{2+}-NFAT pathway. Blocking of CRAC channels drastically decreased recruitment of NFAT and histone modifications within key gene loci involved in Th17 differentiation. The impairment in Th17 differentiation by treatment with CRAC channel blocker was recapitulated in Orai1-deficient T cells, which could be rescued by exogenous expression of retinoic-acid-receptor-related orphan receptors or a constitutive active mutant of NFAT. In vivo administration of CRAC channel blockers effectively reduced the severity of experimental autoimmune encephalomyelitis by suppression of differentiation of inflammatory T cells. These results suggest that CRAC channel blockers can be considered as chemical templates for the development of therapeutic agents to suppress inflammatory responses. ***The Journal of Immunology*****, 2014, 192: 110–122.**

Stimulation of TCR evokes Ca^{2+} entry via Ca^{2+} release–activated Ca^{2+} (CRAC) channels (1). An increase in intracellular Ca^{2+} concentration ($[Ca^{2+}]_i$) induces proliferation and cytokine production in immune cells by activation of downstream target molecules including NFAT (2). The Ca^{2+}-bound calmodulin/calcineurin protein phosphatase complex dephosphorylates heavily phosphorylated, cytoplasmic NFAT, which, in turn, translocates into the nucleus and turns on various transcriptional programs. Orai1 was identified as the pore component of CRAC channels by genome-wide RNA interference (RNAi) high-throughput screens (3–6). Human patients with a homozygous missense mutation in *ORAI1* suffer from lethal SCID (5). Earlier, stromal interaction molecule 1 (STIM1) was identified as an important signaling molecule in the CRAC channel pathway using limited RNAi screens (7, 8). TCR stimulation induces phospholipase C γ–mediated depletion of endoplasmic reticulum (ER) Ca^{2+} stores. STIM1 senses ER Ca^{2+} depletion via its EF hands and translocates into the ER–plasma membrane (PM) junctions to activate Orai1, thereby causing a sustained increase in $[Ca^{2+}]_i$ (7, 9, 10). This sequential activation mechanism was termed store-operated Ca^{2+} entry (SOCE) because depletion of ER Ca^{2+} stores precedes CRAC channel activation (11). Patients with homozygous nonsense mutation in *STIM1* also suffered from SCID, further emphasizing the crucial role of CRAC channels in the immune system (12). Recently, several reports have described the immune phenotypes of Orai1- and STIM1-deficient mice. These mice showed a defect in immune cells, consistent with the SCID patients (13–17).

*Department of Physiology, David Geffen School of Medicine, University of California Los Angeles, Los Angeles, CA 90095; [†]Semel Institute/Department of Psychiatry, David Geffen School of Medicine, University of California Los Angeles, Los Angeles, CA 90095; [‡]California Nanosystems Institute, University of California Los Angeles, Los Angeles, CA 90095; [§]Department of Chemistry and Biochemistry, University of California Los Angeles, Los Angeles, CA 90095; [¶]Division of Hematology-Oncology, David Geffen School of Medicine, University of California Los Angeles, Los Angeles, CA 90095; [‖]University of California Los Angeles AIDS Institute, Los Angeles, CA 90095; and [#]University of California Los Angeles School of Nursing, Los Angeles, CA 90095

[1]K-D.K. and S. Srikanth contributed equally to this work.

Received for publication September 27, 2013. Accepted for publication October 30, 2013.

This work was supported by National Institutes of Health Grants AI-083432 and AI-101569, a grant from the Lupus Research Institute (to Y.G.), and Scientist Development Grant 12SDG12040188 from the American Heart Association (to S. Srikanth). Flow cytometry was performed in the University of California Los Angeles Jonsson Comprehensive Cancer Center Flow Cytometry Core Facility, which is supported by National Institutes of Health Grants CA-16042 and AI-28697.

S. Srikanth and Y.G. designed the research; S. Srikanth performed chemical library screens and human PBMC experiments with technical help from M.-K.Y., M.J., and R.D.; S. Srikanth and B.R. performed and analyzed patch-clamp experiments; K.-D.K. analyzed T cell phenotypes and performed experimental autoimmune encephalomyelitis experiments with Y.-V.T. under the guidance of J.A.W.; M.E.J. contributed to chemical designing; D.S.A. and S. Shimizu assisted in human PBMC experiments; S. Srikanth, K.-D.K., and Y.G. wrote the manuscript; and Y.G. supervised the project.

Address correspondence and reprint requests to Prof. Yousang Gwack, Department of Physiology, David Geffen School of Medicine, University of California Los Angeles, 53-266 CHS, 10833 Le Conte Avenue, Los Angeles, CA 90095. E-mail address: ygwack@mednet.ucla.edu

The online version of this article contains supplemental material.

Abbreviations used in this article: $[Ca^{2+}]_i$, intracellular Ca^{2+} concentration; CA-NFAT, constitutively active NFAT; ChIP, chromatin immunoprecipitation; CRAC, Ca^{2+} release–activated Ca^{2+}; CsA, cyclosporine A; C_T, threshold cycle; EAE, experimental autoimmune encephalomyelitis; MEF, murine embryonic fibroblast; MOG, myelin oligodendrocyte glycoprotein; NFAT-GFP, NFATc2-1-460–GFP; PM, plasma membrane; RNAi, RNA interference; ROR, retinoic acid receptor–related orphan receptor; SOCE, store-operated Ca^{2+} entry; STIM1, stromal interaction molecule 1; TIRF, total internal reflection fluorescence; TIRFM, total internal reflection fluorescence microscopy; Treg, regulatory T cell; WT, wild-type.

Upon stimulation, naive $CD4^+$ T cells differentiate into distinct effector cell types including Th1, Th2, and Th17 cells. Accumulating data suggest that Th17 cells are highly proinflammatory and are essential for severe autoimmunity in various disease models including a murine model of multiple sclerosis, experimental autoimmune encephalomyelitis (EAE). During differentiation of Th17 cells, cytokines including IL-1, IL-6, IL-21, IL-23, and TGF-β promote IL-17 production and expression of lineage-specific transcription factors including retinoic acid receptor–related orphan receptor γt (RORγt) and RORα (18–23). Individual or combined deletion of RORγt and RORα drastically reduced Th17 cell differentiation, and accordingly, these mice showed a strong resistance to EAE (24).

In Th1-Th2 paradigm, it is well-known that TCR signaling contributes to the differentiation of naive T cells into lineage-specific effector T cells. Previous studies have shown that the strength of TCR stimulation plays an important role in lineage specification, with stronger stimulation favoring differentiation into Th1 cells and weaker stimulation favoring Th2 differentiation (25). In the case of Th17 cells, it is known that TCR stimulation in conjunction with cytokines is crucial for differentiation (21–23). However, the contribution of TCR stimulation-induced Ca^{2+} signaling pathway underlining Th17 differentiation remains poorly understood, partly because of the recent identification of Orai1 and STIM1.

Using genome-wide RNAi screens in *Drosophila* cells that used NFATc2-1-460–GFP (NFAT-GFP) translocation to the nucleus as readout, we identified two novel families as regulators of NFAT, dual-specificity tyrosine-regulated kinases and Orai Ca^{2+} channels (5, 6, 26). In this study, we extended a similar strategy to chemical library screens using a mammalian cell line exhibiting amplified CRAC channel activity. High-throughput screening from a total of ∼85,000 chemicals led to identification of a novel class of small-molecule compounds as CRAC channel inhibitors. Treatment with these compounds strongly blocked differentiation of Th17 cells in vitro and in vivo with higher sensitivity when compared with Th1 and Th2 cells. At a molecular level, treatment with one of the blockers, compound 5D, reduced expression levels of RORα and RORγt transcription factors during Th17 differentiation, and this defect was rescued by overexpression of RORα, RORγt, and a constitutively active mutant of NFAT. Furthermore, treatment with compound 5D strongly reduced active chromatin marks of RORα, RORγt, and IL-17 promoters. These results reveal a direct role of the Orai-NFAT pathway in regulation of RORα and RORγt expression during Th17 differentiation. Our study suggests that derivatives of compound 5D can be used as chemical templates for the development of therapeutic agents to alleviate inflammation and as molecular probes to investigate the role of TCR stimulation-mediated Ca^{2+} entry in inflammatory diseases.

Materials and Methods

Reagents and Abs

Thapsigargin and 2-APB were purchased from EMD Chemicals (Billerica, MA). The following Abs were obtained from eBioscience (San Diego, CA) and used for surface and intracellular staining: CD4 (GK1.5), IL-4 (11B11), IFN-γ (XMG1.2), IL-17A (eBio17B7), and RORγt (AFKJS-9).

Plasmids

Full-length cDNA of human Orai1 was subcloned into bicistronic retroviral expression vector pMSCV-CITE-eGFP-PGK-Puro (which allows for simultaneous expression of Orai1, GFP, and a puromycin resistance gene) and has been described previously (27). Single-point mutants were generated using Quickchange XL site-directed mutagenesis kit (Stratagene, Santa Clara, CA) following manufacturer's instructions. All the clones were verified by sequencing. For total internal reflection fluorescence (TIRF) analysis, wild-type (WT) Orai1 cDNA was fused in-frame with pEGFP to have a C-terminal GFP-tag. STIM1-mCherry plasmid has been described previously (27, 28). Orai1 $Q^{108}LD^{110}\rightarrow A^{108}AA^{110}$ and $D^{110}AD^{112}>A^{110}AA^{112}$ were generated by introducing an NotI site in the primers. Orai1 ΔEC2 clone was generated by deletion of aa L^{202}–P^{231} within the second extracellular loop by introduction of an NotI restriction enzyme site.

Cell lines and transductions

HEK293 cells were obtained from American Type Culture Collection and cultured in DMEM (Mediatech, Hargrave, VA) supplemented with 10% FBS (Hyclone, Logan, UT), 10 mM HEPES, 10 mM glutamine, and 1% penicillin/streptomycin (Mediatech, Hargrave, VA). Cells were transfected at 60–70% confluency using Lipofectamine 2000 (Invitrogen, Carlsbad, CA) according to the manufacturer's instructions. For retroviral transductions, phoenix cells stably expressing gag-pol and ecotropic env (purchased from American Type Culture Collection) were transfected with plasmids encoding Orai cDNAs to produce ecotropic, replication-incompetent retrovirus using calcium phosphate transfection method. Virus-containing supernatant was collected at 2 and 3 d after transfection, and immortalized $Orai1^{-/-}$ murine embryonic fibroblasts (MEFs) (13) or primary T cells were transduced in the presence of 8 μg/ml polybrene. Transduction efficiencies were evaluated visually by GFP expression.

High-throughput screen to identify small-molecule blockers of CRAC channels

HeLa cells stably expressing Orai1, STIM1, and NFAT-GFP were generated by retroviral transduction with viruses encoding each cDNA and antibiotic selection. Cells were FACS-sorted for selection of GFP^{high} population. Approximately 5000 cells were plated onto individual 384-well plates coated with poly-L-lysine (Greiner Bio-one, Monroe, NC). The next day, the cells were washed twice with 2 mM Ca^{2+}-containing Ringer solution and bathed in the same solution. Compounds were added using a 384-well pin tool (V&P Scientific, San Diego, CA) at a final concentration of 10 μM. Cells were incubated with the compounds for 5 min and then treated with a final concentration of 1 μM thapsigargin for ∼30 min, fixed, permeabilized, and stained with DAPI, and the coincident GFP and DAPI images were acquired by an automated camera from each well. Every plate included two type of controls: one without any compound to monitor nuclear translocation of NFAT-GFP and another with 100 μM 2-APB to visualize block of NFAT-GFP nuclear translocation. Only the plates showing expected patterns for control wells were used for further evaluation. The chemical libraries of Biomol, FDA-approved drugs, MicroSource, Prestwick, Chembridge, Druggable compounds, and leadlike compounds totaling to ∼85,000 small-molecule compounds were used in the primary screen. Candidates from the primary screen were cherry-picked into 96-well plates, and a confirmatory screen was performed in triplicates using the protocol described earlier. Positive candidates from the confirmatory screen were then examined for their blocking efficacy on SOCE using single-cell Ca^{2+} imaging.

Single-cell Ca^{2+} imaging

HeLa O+S cells and fibroblasts were grown directly on UV-sterilized coverslips and loaded with 2 μM Fura 2-AM for 45 min. Primary T cells were loaded with 1 μM Fura 2-AM for 30 min and attached onto poly-D-lysine–coated coverslips. For $[Ca^{2+}]_i$ measurements, cells were mounted on a RC-20 closed bath flow chamber (Warner Instrument, Hamden, CT) and analyzed on an Olympus IX51 epifluorescence microscope with Slidebook (Intelligent Imaging Innovations) imaging software. Cells were perfused with Ca^{2+}-free Ringer's solution, and Ca^{2+} stores were passively depleted with 1 μM thapsigargin. SOCE was measured by exchanging the Ca^{2+}-free Ringer's solution with that containing 2 mM $CaCl_2$. At the peak of SOCE, cells were exposed to the same solution containing 10 μM (or different concentrations) of individual blockers. Fura-2 emission was detected at 510 nm with excitation at 340 and 380 nm, and the Fura-2 emission ratio (340/380) was acquired at every 5-s interval after background subtraction. For each experiment, 50–100 individual cells were analyzed using OriginPro (Originlab, Northampton, MA) analysis software. Peak-basal Ca^{2+} ratio was calculated after subtracting the ratio value after store depletion, before reintroduction of Ca^{2+} containing Ringer's solution from the maximal value of 340/380 ratio after reintroduction of Ca^{2+} containing Ringer's solution. Sustained Ca^{2+} was calculated as the 340/380 ratio at the time point of 800 s after subtracting basal Ca^{2+} ratio.

TIRF microscopy analysis

HEK293 cells were transfected with plasmids encoding STIM1-mCherry along with WT Orai1-GFP fusion protein encoding cDNAs at a molar ratio of 1:1. TIRF microscopy (TIRFM) was performed using an Olympus

IX2 illumination system mounted on an Olympus IX51 inverted microscope. Laser beams from a 488-nm argon ion laser (Melles Griot, Carlsbad, CA) and a 594-nm diode laser (Cobolt Instruments, San Jose, CA) were combined and controlled using an Olympus OMAC TIRF dual-port condenser and controller system. The angle of the incident light at the interface between the glass coverslip and the aqueous medium was controlled by independently adjusting the position of each laser beam before passing through a 60× oil-immersion objective (NA 1.49; Olympus). The emission was filtered either at D525/50 or 660/50 nm filter (Chroma Technology, Bellows Falls, VT) and captured by a Hamamatsu ORCA cooled CCD (Roper Scientific, Tucson, AZ) camera. Acquisition and image analysis were performed using Slidebook (Intelligent Imaging Innovations, Denver, CO) and OriginPro8.5 software.

Measurement of CRAC currents by whole-cell recording

For recording of CRAC currents, HEK293 cells were cotransfected with plasmids encoding Orai1 WT or mutant cDNAs in the presence or absence of STIM1 encoding plasmid at a molar ratio of 1:1 using Lipofectamine 2000 (Invitrogen, Carlsbad, CA). Cells were used for experiments 24-48 h post transfection. Patch-clamp recordings were performed using an Axopatch 200B amplifier (Molecular Devices, Sunnyvale, CA) interfaced to a Digidata 1320A (Molecular Devices, Sunnyvale, CA) for stimulation and data acquisition. Currents were filtered at 1 kHz with a four-pole Bessel filter and sampled at 5 kHz. Recording electrodes were pulled from borosilicate glass capillaries (WPI, Sarasota, Fl) using a Flaming Brown pipette puller (Sutter Instrument, Novato, CA) to a final resistance of 2–7 MΩ. Stimulation, data acquisition, and analysis were performed using pCLAMP8 and Origin software. The standard extracellular Ringer's solution contained (in mM): 145 Cs-aspartate, 4.5 KCl, 6 $CaCl_2$, 10 D-glucose, and 10 Na-Hepes (pH 7.35). The standard internal solution contained (in mM): 145 Cs-glutamate, 8 $MgCl_2$, 12 EGTA, and 10 Cs-Hepes (pH 7.3). Unless otherwise stated, the cell membrane was held at 0 mV, and pulses were applied between −110 and +115 mV at 15-mV intervals for 250 ms.

Analysis of patch-clamp data

Ionic currents from cells expressing WT and mutant channels were recorded using only the analog compensation of the membrane linear components. In some cases (mutant channels), the blocker(s) had no inhibitory effects and the current traces could not be corrected for leak currents. The first 1 ms of recorded data after the onset of the voltage pulses was not included in the fitting to minimize the effect of uncompensated membrane capacitance on the estimated time course of the current. For the I-V, steady-state currents measured at the end of the pulse were used.

T cell isolation and differentiation

$CD4^+$ T cells were purified from single-cell strained suspensions prepared by mechanical disruption of spleens and lymph nodes of adult mice after magnetic sorting with $CD4^+$ beads (Invitrogen). $CD4^+CD25^-$ naive T cells were selected by CD25 MACS positive selection (Miltenyi Biotec, Auburn, CA). For effector T cell differentiation, cells were stimulated with 2 μg/ml anti-CD3 (Bio X cell, West Lebanon, NH) and anti-CD28 (Bio X cell, West Lebanon, NH) Abs for 48 h on a plate coated with 0.1 mg/ml goat anti-hamster (MP Biomedicals, Solon, OH). $CD4^+CD25^-$ T cells were cultured with 10 μg/ml anti–IL-4 (Bio X cell) and 10 ng/ml IL-12 for Th1 differentiation, 20 μg/ml anti–IFN-γ (Bio X cell, West Lebanon, NH), 2.5 μg/ml anti–IL-12, and 10 ng/ml IL-4 (Peprotech, Rocky Hill, NJ) for Th2 differentiation, and 10 μg/ml anti–IL-4, 20 μg/ml anti–IFN-γ, 30 ng/ml IL-6 (Peprotech), 3 ng/ml TGF-β (Peprotech), and 10 ng/ml IL-23 (R&D Systems, Minneapolis, MN) for Th17 differentiation. On day 4, differentiated T cells were restimulated with 20 nM PMA and 1 μM ionomycin for cytokine analysis.

Active EAE induction in mice

All animals were maintained in pathogen-free barrier facilities and used in accordance with protocols approved by the Institutional Animal Care and Use Committee at the University of California Los Angeles (UCLA). For induction of EAE, mice were immunized s.c. on day 0 with 100 μg myelin oligodendrocyte glycoproteins 35–55 ($MOG_{35–55}$) peptide (N-MEVGWYRSPFSRVVHLYRNGK-C; Genscript) emulsified in CFA (Difco, Houston, TX) supplemented with 5 mg/ml *Mycobacterium tuberculosis* H37Ra (Difco, Houston, TX). These mice were also injected i.p. with 200 ng/mouse pertussis toxin (List Biological Laboratories, Campbell, CA) on days 0 and 2. EAE was scored according to the following clinical scoring system: 0, no clinical signs; 1, limp tail; 2, partial hind-leg paralysis; 3, complete hind-leg paralysis or partial hind- and front-leg paralysis; 4, complete hind- and partial front-leg paralysis. Mice were injected i.p. with either the vehicle (DMSO, 50 μl), compound 5D (1 mg/kg), or 5J-4 (2 mg/kg) every alternate day starting from day 0.

T cell analysis

Draining lymph nodes were collected 14 d after EAE induction, and cell suspensions were prepared. For proliferation analysis, cells were distributed in a 96-well plate at 1×10^6 cells/ml concentration and cultured in media. Cell suspensions were restimulated with 20 μg/ml $MOG_{35–55}$ for 2 d at 37°C with 5% CO_2 and humidified atmosphere. All the cultures were run in triplicates. After 48 h, cultures were pulsed with 1 μCi/well [^{3}H]thymidine (Amersham Biosciences, Piscataway, NJ) for an additional 16–18 h. After this treatment, cells were harvested, lysed, and acid precipitated. Finally, [^{3}H]thymidine incorporation was determined by liquid β-scintillation counting (Beckman Coulter, Brea, CA). For intracellular staining, cells were distributed in a 12-well plate at 1×10^6 cells/ml concentration and cultured with 20 nM PMA and 1 μM ionomycin for 5 h. For real-time PCR, the total RNA of draining lymph nodes was extracted with TRIzol reagent (Invitrogen, Carlsbad, CA) following the manufacturer's instructions. For ex vivo experiments, draining lymph nodes were collected 7 d after EAE induction, and cell suspensions were prepared. Cells were distributed in a 12-well plate at 1×10^6 cells/ml concentration and cultured for 4 more days with the MOG peptide (20 μg/ml) together with exogenous IL-6 and IL-23 or IL-12, in the presence or absence of compound 5D.

Isolation of mononuclear cells from the CNS

Tissues were digested in collagenase and DNase I (Roche) for 30 min at 37°C, and cells were separated on a 40–80% Percoll gradient by centrifugation at 500 × *g* for 30 min. Cells at the 40–80% interface were collected to isolate mononuclear cells from PBS-perfused spinal cords and brain. For intracellular cytokine staining, cells were stimulated with 20 nM PMA and 1 μM ionomycin in the presence of 3 μg/ml brefeldin A (eBioscience, San Diego, CA) for 5 h and stained for CD4, IFN-γ, and IL-17A.

Histology

After perfusion with PBS, spinal cords were removed and fixed with 4% paraformaldehyde in PBS at 4°C overnight. Tissues were blocked in paraffin wax. Sections (5 μm) were cut from paraffin block. Paraffin-embedded sections were stained with H&E and Luxol fast blue for visualization of inflammatory infiltrates and demyelination.

Real-time quantitative PCR

cDNA was synthesized from total RNA using oligo(dT) primers and Superscript III First-Strand cDNA synthesis kit (Invitrogen). Real-time PCR was performed using an iCycler IQ5 system (Bio-Rad) and SYBR Green dye (Sigma) using the primers described in Supplemental Table I. Threshold cycles (C_T) for all the candidate genes were normalized to the C_T values for β-actin housekeeping gene control to obtain ΔC_T. The specificity of primers was examined by melt-curve analysis and agarose gel electrophoresis of PCR products.

Chromatin immunoprecipitation

After culturing naive T cells under Th17-polarizing conditions with plate-coated anti-CD3 and anti-CD28 Abs for 16 h, cells were fixed for 8 min at room temperature with 1:37 dilution of 37.1% formaldehyde (Calbiochem), neutralized with 1:20 dilution of 2.5 M glycine, and washed twice in ice-cold PBS. Cells were lysed in 500 μl low-salt buffer (0.1% SDS, 1% Triton X-100, 2 mM EDTA, 20 mM Tris-HCl, pH 8.1, 150 mM NaCl) and chromatin sheared by sonication to generate 200–800 bp DNA fragments. For immunoprecipitation with anti–acetyl-histone H3-K14 (catalog no. 07-353; Millipore), anti–acetyl-histone H3-K9 (catalog no. 07-352; Millipore), and anti-NFAT1 Ab (clone 67.1), chromatin from 1×10^7 whole-cell equivalents was used. Chromatin was diluted in low-salt washing buffer, and immunoprecipitation was performed by overnight incubation with the indicated Abs, followed by 2-h (at 4°C) incubation with 3 μg protein A-Sepharose CL-4B (GE Healthcare). Immunocomplexes were captured and washed twice for 5 min each with low-salt washing buffer, high-salt washing buffer (0.1% SDS, 1% Triton X-100, 2 mM EDTA, 20 mM Tris-HCl, pH 8.1, 500 mM NaCl), LiCl washing buffer (0.25 M LiCl, 1% Nonidet P-40, 0.1% deoxycholate, 1 mM EDTA, 10 mM Tris 8.1), and TE buffer (Tris-HCl 10 mM, EDTA 1 mM). Beads were resuspended in TE and then treated with 5 μl of 1 mg/ml RNase A for 30 min at 37°C and, finally, with proteinase K (0.2 mg/ml; Roche) overnight at 37°C. The samples were heated to reverse cross-linking at 65°C

overnight. DNA was purified using phenol-chloroform extraction and ethanol precipitation. Selected DNA sequences were quantified by real-time quantitative PCR using primers described in Supplemental Table I. Chromatin immunoprecipitation (ChIP) data are presented as the percentage recovery of input.

Human PBMC culture

Mononuclear cells were prepared from buffy coats from healthy, unidentified adult donors, obtained under federal and state regulations from the UCLA CFAR Gene and Cellular Therapy Core Laboratory. PBMCs were activated with anti-CD3/CD28 beads (Miltenyi Biotech) and cultured in T cell media (DMEM containing 20% FBS and 1% Pen-Strep) supplemented with 20 U/ml IL-2 (Peprotech), 10 ng/ml IL-1β, and 10 ng/ml IL-23 (eBioscience) in the presence or absence of 20 μM compound 5D. Cells were expanded with fresh media, cytokines, and compound 5D every alternate day. On day 6, cells were extensively washed and activated with 20 nM PMA, 1 μM ionomycin, and brefeldin A (3 μg/ml) for 5 h, surface stained with anti–CD4-FITC, and intracellularly stained with anti–IL-17A–allophycocyanin and anti–IFN-γ–PE. CD4-FITC$^+$ cells were gated for analysis. For flow cytometry, the following human specific Abs were used: CD4-FITC (OKT4; eBioscience), IL-17A–allophycocyanin (eBio64CAP17; eBioscience), and IFN-γ–PE-Cy7 (45.B3; eBioscience).

Statistical analysis

Statistical analysis was carried out using two-tailed Student *t* test. Differences were considered significant when p values were < 0.05.

Results

Identification of a small-molecule blocker of Orai1, compound 5 from a chemical library screen

To develop a high-throughput screen to identify Orai1 inhibitors, we generated a cell line in which the CRAC currents (I_{CRAC}) are amplified by stable expression of Orai1 and STIM1 (27). A pilot screen using direct measurement of cytoplasmic Ca^{2+} concentration ($[Ca^{2+}]_i$) provided a Z′ factor of ∼0.5. Earlier, using NFAT translocation as readout for CRAC channel activity in *Drosophila* cells, we specifically selected ∼20 candidates from a genome-scale RNAi screen (5, 6). Therefore, we generated HeLa-O+S cells stably expressing NFATc2 (aa 1–460)-GFP (abbreviated NFAT-GFP) to use nuclear translocation of NFAT-GFP as readout (Fig. 1A). Nuclear translocation of NFAT in HeLa-O+S cells triggered by store depletion was suppressed by blocking CRAC channels with 2-APB, suggesting that it is predominantly regulated by CRAC channel activity. A pilot screen using NFAT translocation as readout showed a Z′ factor of ∼0.7, providing an ideal platform for high-throughput screening. A chemical library encompassing ∼85,000 compounds was screened to identify blockers of NFAT translocation. Each plate included a positive control, 2-APB, and plates were automatically scored for colocalization of NFAT-GFP and DAPI signals. Candidates affecting survival or morphology of the cells were excluded from further analyses. Positive candidates from the primary screen were further examined for direct block of SOCE using single-cell ratiometric Ca^{2+} imaging. This analysis resulted in identification of compound 5, *N*-[2,2,2-trichloro-1-(1-naphthylamino)ethyl]-2-thiophenecarboxamide, as a specific inhibitor of CRAC channels (Fig. 1B).

A structural analog of compound 5 potently blocks CRAC channel activity

To identify compounds with better blocking efficacy, we examined structural analogs of compound 5 for block of SOCE in HeLa-O+S cells. Among these, compound 5D, *N*-[2,2,2-trichloro-1-(2-naphthylamino)ethyl]-2-furamide, showed an enhanced block of SOCE (Fig. 1B, Supplemental Fig. 1A). Modifications in the structure of the thiophene or naphthalene rings of compound 5 reduced the blocking effect, suggesting their important role in inhibiting CRAC channel activity (data not shown). We next examined the blocking efficacy of compound 5D on endogenous CRAC channels in primary CD4$^+$ T cells. Compound 5D blocked endogenous SOCE, especially sustained Ca^{2+} levels of effector T cells, in a dose-dependent manner with a half-maximum inhibitory concentration of 807 and 195 nM for the peak and sustained levels of SOCE, respectively (Fig. 1C).

Compound 5D inhibits CRAC channel activity by blocking ion permeation

The CRAC channel has unique gating and inactivation mechanisms. ER store depletion induces multimerization and clustering of STIM1 at the ER–PM junctions, which allows for a direct protein interaction between Orai1 and STIM1 (1). To elucidate the molecular mechanism of inhibition by compound 5D, we measured the effect of compound 5D at different stages of Orai1 activation. First, we examined whether presence of compound 5D altered accumulation of STIM1 and Orai1 at the ER–PM junctions using TIRFM. These studies showed no significant effect of compound 5D on the rate or extent of accumulation of Orai1 or STIM1 at the ER–PM junctions (Supplemental Fig. 1B). Next, to examine the effect of compound 5D on CRAC currents, we used HEK293 cells transiently expressing Orai1 and STIM1. In these cells, we could detect large I_{CRAC} that was almost completely blocked by compound 5D when applied in the external solution, whereas intracellular application via the patch pipette had no effect (Fig. 1D). These results suggested that the binding site of compound 5D is located at or near the extracellular region of Orai1.

Orai1 contains four transmembrane segments (TM1–4), cytoplasmic N and C termini, and two extracellular loops EC1 and EC2 with TM1 lining the pore (Fig. 1E). Recently, we showed that the mutation W176C in TM3 resulted in STIM1-independent, constitutively active CRAC currents (29). Compound 5D could reversibly inhibit currents generated from Orai1^{W176C} (Fig. 1F, Supplemental Fig. 1C), suggesting that blocking by compound 5D is independent of STIM1 interaction with Orai1. Previous mutational analysis of transmembrane segments of Orai1 suggested that residues L95, G98, and V102 in TM1 segment of Orai1 are directly involved in ion permeation (30, 31). Because Orai1 inhibitor compound 5D blocks CRAC currents when applied extracellularly, we mutated conserved residues in the two EC loops, as well as in TM1, that can be accessible from the extracellular milieu when the channel is open. Various mutants of Orai1 in TM1 and two EC loops were expressed in Orai1$^{-/-}$ MEFs and examined for block of SOCE (Fig. 1F). It has been suggested that extracellular loop 1, which contains three aspartate residues ($D^{110}\times D^{112}\times D^{114}$), forms the channel's outer vestibule and is possibly involved in ion selectivity (1). Mutation of these residues (mutants $Q^{108}LD^{110}>AAA$ and $D^{110}AD^{112}>AAA$) did not affect blocking by compound 5D. In addition, deletion of extracellular loop 2 (ΔEC2) also did not affect block by compound 5D. Recent studies suggested that residue V102 within TM1 may form the gate that opens and closes CRAC channels, and its mutation results in STIM1-independent and constitutively active channels (32). Our mutational analysis of this residue demonstrated a very slow and partial block of Orai1^{V102C}- and Orai1^{V102A}-evoked currents by compound 5D (Fig. 1F, Supplemental Fig. 1D, 1E). These data suggest that compound 5D specifically blocks Orai family of channels by binding at or near V102 (of Orai1) to close the channel, although we cannot rule out the possibility of its binding

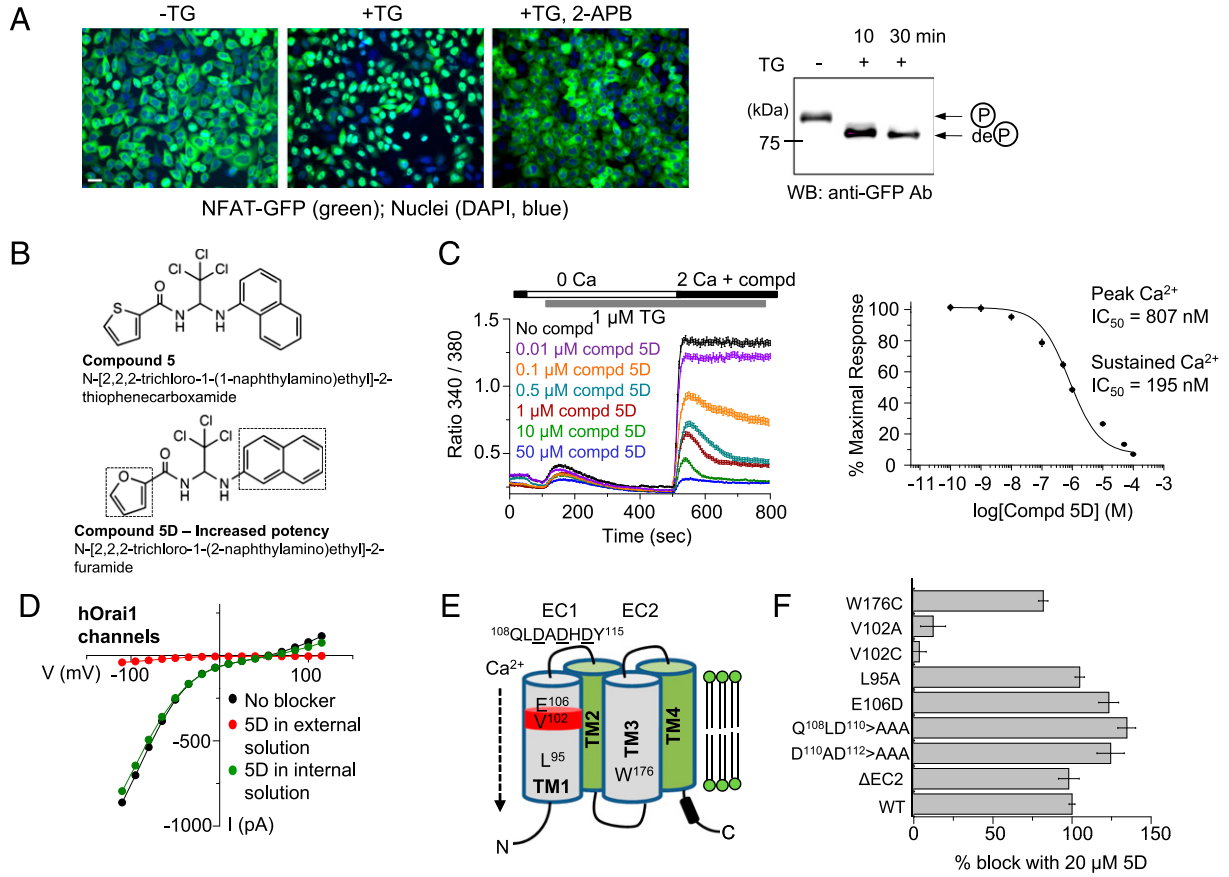

FIGURE 1. Identification of compound 5D as a small-molecule blocker of CRAC channels. (**A**) Development of NFAT translocation as readout for high-throughput screen. HeLa cells stably expressing Orai1, STIM1, and NFAT-GFP were left untreated (−TG) or treated with thapsigargin (+TG; 1 μM, 30 min) with and without 2-APB. The cells were examined by microscopy for nuclear accumulation of NFAT-GFP (*left panels*) or immunoblotting for dephosphorylation of NFAT with anti-GFP Ab (*right panel*). Scale bar, 10 μm. (**B**) Chemical structures of compound 5 and its structural analog compound 5D. (**C**) Dose-dependent block of endogenous SOCE in primary murine effector T cells cultured under nonskewing conditions after exposure to compound 5D. Each trace represents average ± SEM from 50–60 primary T cells. The right graph shows dose-dependent block of sustained $[Ca^{2+}]_i$ by compound 5D with the indicated half-maximum inhibitory concentration (IC_{50}). (**D**) Inhibition of CRAC currents by compound 5D. Measurement of CRAC currents from HEK293 cells coexpressing Orai1 and STIM1 (black trace). Cells were exposed to compound 5D (10 μM) by either intracellular (green trace) or extracellular (red trace) application. Representative I-V from at least four different cells in each condition is depicted. (**E**) Schematic of Orai1. Orai1 contains four transmembrane segments (TM1–TM4) with its N and C termini facing the cytoplasm, and two extracellular loops (EC1 and EC2). Residues L95, V102, and E106 in TM1 directly line the ion permeation pathway, and V102 has been proposed to form the gate of the CRAC channel (marked in red). The $D^{110}\times D^{112}\times D^{114}$ motif in the EC1 is important for ion selectivity of the channel, and mutation of W176 in TM3 makes the channel constitutively open. (**F**) Compound 5D–mediated block of SOCE induced by various mutants of Orai1. SOCE measurements and its block by compound 5D from $Orai1^{-/-}$ MEFs transduced with retroviruses encoding either WT or indicated mutants of Orai1. Residues deleted in the second extracellular loop (ΔEC) are described in *Materials and Methods*. Data represent average ± SEM from 25–35 fibroblasts and are normalized to the block of WT Orai1. The blocking effect of compound 5D on constitutively active channels such as W176C, V102A, and V102C was measured without store depletion. deP, Dephosphorylated; P, phosphorylated; WB, Western blotting.

to a remote site and allosterically causing closure of the channel gate at V102.

Compound 5D did not have any effect on Ca^{2+} entry mediated by TrpC1 (transient receptor potential canonical) channels, a member of TrpC family of store-operated Ca^{2+} channels, when coexpressed with STIM1 in HEK293T cells (Supplemental Fig. 1F). To examine whether compound 5D blocked SOCE via other Orai proteins, we transduced Orai1-deficient T cells with retroviruses for expression of Orai2 and Orai3 proteins (13). We observed block of residual SOCE in Orai1-deficient T cells, which is likely to be mediated by Orai2 or Orai3 proteins (Supplemental Fig. 1G) (13, 33). Expression of all the Orai proteins enhanced SOCE in Orai1-deficient T cells, supporting earlier observation that all three Orai proteins can be activated by store depletion (34, 35). Importantly, compound 5D treatment blocked SOCE mediated by all three Orai proteins (Supplemental Fig. 1G). Collectively, our results suggest that compound 5D specifically blocks Orai proteins by binding to a site facing the extracellular milieu, and its inhibitory mechanism involves the potential channel gate located at V102.

Th1, Th2, and Th17 differentiation exhibit different sensitivity to CRAC channel inhibition

To analyze the effect of compound 5D on SOCE in various T cells, we measured SOCE from naive and stimulated murine T cells cultured under Th1-, Th2-, and Th17-polarizing conditions. Although compound 5D blocked SOCE in Th1, Th2, as well as Th17 cells, the block was stronger for differentiated Th17 cells when compared with that of naive, Th1, or Th2 cells (Fig. 2A). Consistent with these results, IL-17A production by Th17 cells was more severely affected when compared with IFN-γ and IL-4 production by Th1 and Th2 cells, respectively, in the presence

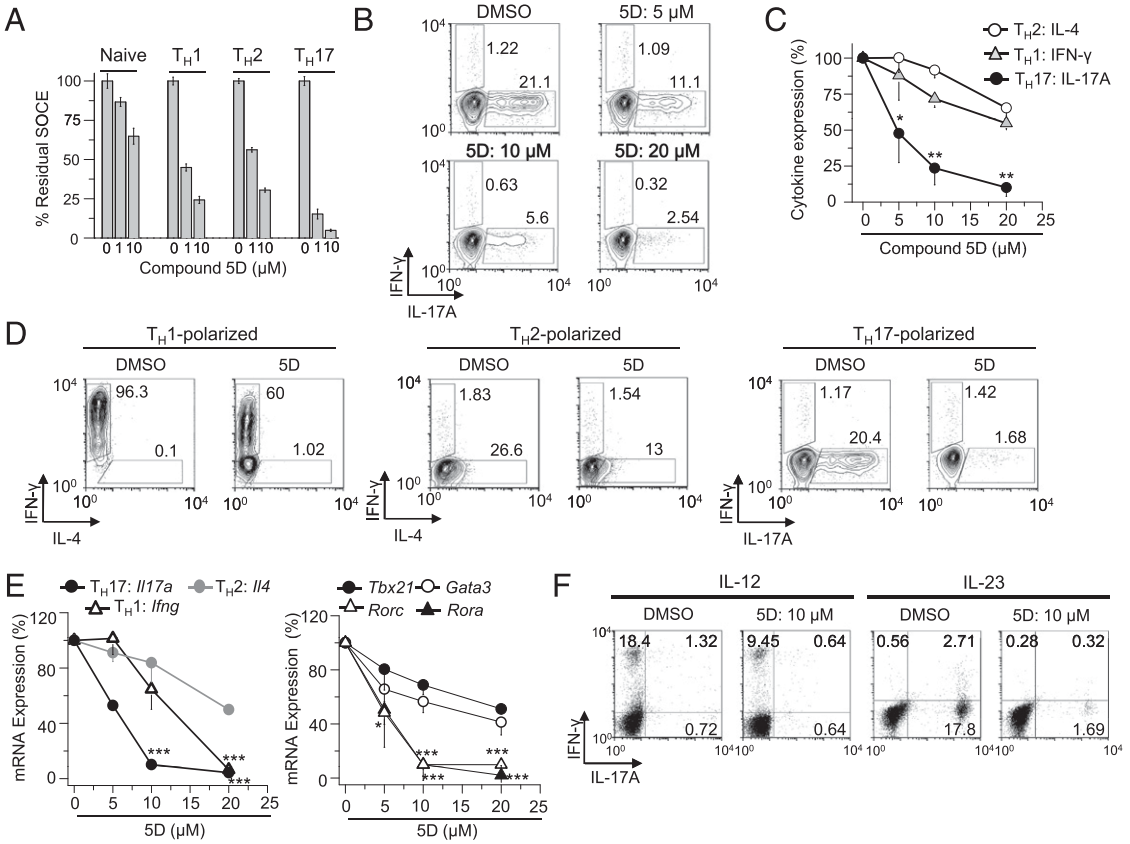

FIGURE 2. Inhibition of CRAC channels reduces differentiation of effector T cells. (**A**) Measurement of SOCE in naive and indicated effector T cells in the absence and presence of 1 or 10 μM compound 5D. Data represent average ± SEM of peak SOCE from 40 to 60 cells and are normalized to SOCE in the absence of compound 5D. (**B**) Compound 5D–mediated inhibition of IL-17A production. Naive T cells differentiated under Th17-polarizing conditions and restimulated with PMA and ionomycin with different concentrations of compound 5D or DMSO (vehicle) were examined for IL-17A and IFN-γ production. (**C**) Compound 5D–mediated inhibition of cytokine production by Th1, Th2, and Th17 cells. Naive T cells differentiated under Th1-, Th2-, or Th17-polarizing conditions were stimulated with PMA and ionomycin after 4 d in the presence of different concentrations of compound 5D and examined for cytokine expression using intracellular staining. Data were normalized to cytokine levels of cells treated with DMSO. $*p < 0.05$, $**p < 0.0005$. (**D**) Compound 5D affects T cell differentiation. Naive T cells differentiated under Th1-, Th2-, and Th17-polarizing conditions in the absence or presence of compound 5D (15 μM) for 4 d were restimulated with PMA and ionomycin for 6 h in the absence of compound 5D and stained for IFN-γ, IL-4, and IL-17A, respectively. (**E**) Compound 5D–mediated reduction in the expression of cytokines and transcription factors in T cells. Naive T cells differentiated under Th1-, Th2-, and Th17-polarizing conditions with compound 5D were washed, restimulated with PMA plus ionomycin, and harvested for mRNA expression analyses of IFN-γ (Th1 cells), IL-4 (Th2 cells), and IL-17A (Th17 cells) (*left panel*). In addition, the mRNA levels of T-bet, GATA-3, RORγt, and RORα were also measured under Th1-, Th2-, and Th17-polarizing conditions, respectively (*right panel*). $*p < 0.05$, $***p < 0.0005$. (**F**) Compound 5D–mediated block of expansion and maintenance of predifferentiated Th17 cells. Cells were collected from draining lymph nodes of mice 7 d after immunization with $MOG_{35–55}$/CFA and cultured for 4 d with $MOG_{35–55}$ peptide together with IL-12 or IL-23 in the presence of DMSO or 10 μM compound 5D. $CD4^+$ T cells were examined for IL-17A and IFN-γ production after stimulation with PMA and ionomycin.

of compound 5D (Fig. 2B, 2C). Next, to determine the effect of inhibition of SOCE on T cell differentiation, we stimulated naive T cells under Th1-, Th2-, and Th17-polarizing conditions in the presence and absence of compound 5D. In these experiments, compound 5D was included specifically during the differentiation stage but excluded during restimulation to examine cytokine production. Presence of compound 5D during differentiation blocked cytokine production by Th1, Th2, as well as Th17 cells; however, Th17 cells showed a stronger block of IL-17A production when compared with IFN-γ and IL-4 production by Th1 and Th2 cells, respectively (Fig. 2D). Analysis of lineage-specific cytokines and transcription factors showed a pronounced reduction of mRNA levels of IL-17A, RORα, and RORγt under Th17-polarized conditions even with low concentrations of compound 5D, compared with those of IFN-γ and T-bet under Th1-polarized conditions, or IL-4 and GATA-3 under Th2-polarized conditions (Fig. 2E). Contrary to Th17 cells, differentiation of inducible regulatory T cells was not significantly influenced by treatment with compound 5D as judged by expression levels of Foxp3 (Supplemental Fig. 2A). Previous studies have shown that Th17 cells have a distinct Ca^{2+} profile when compared with Th1 and Th2 cells (36). Because Th17 cells showed higher sensitivity to block by compound 5D, and the role of SOCE and NFAT family of transcription factors in differentiation of Th17 cells is less understood, we focused our studies on Th17 cells. We observed reduced expression levels of molecules involved in Th17 pathogenicity including IL-23R, CCR6, and integrin αL (LFA-1) in compound 5D–treated cells (Supplemental Fig. 2B). Although inhibition of CRAC channel activity by compound 5D decreased induction levels of NFATc1/αA that depends on Ca^{2+}-NFAT signaling pathway as expected (37), it did not significantly alter mRNA expression levels of other transcription factors including c-Maf, Runt-related transcription factor 1, aryl hydrocarbon receptor, IFN-regulatory factor 4, suppressor of cytokine signaling 3, IκBζ, basic leucine zipper transcription factor ATP-like, or hypoxia-inducible factor 1, all of which are known to play an important role in Th17 differentiation (Supplemental Fig. 2C) (38–44). These data suggest a selective role of Orai1-mediated

Ca^{2+} signaling in regulating the expression levels of RORα and RORγt during Th17 differentiation.

Next, we investigated whether compound 5D inhibits in vitro expansion/maintenance of Ag-specific effector T cells. For these experiments, WT mice were injected with a peptide derived from MOG ($MOG_{35–55}$ peptide) emulsified with CFA, and after 7 d, draining lymph nodes were harvested. Cells from the draining lymph nodes were cultured with $MOG_{35–55}$ peptide plus exogenous IL-12 or IL-23 with or without compound 5D, and examined for IFN-γ– and IL-17A–producing populations. We observed reduction of both IFN-γ and IL-17A in compound 5D–treated cells; however, the reduction of IL-17A–producing cells was more pronounced (Fig. 2F). These experiments suggested that in addition to de novo differentiation, expansion/maintenance of pre-differentiated Th17 cells also needed CRAC channel activity.

Expression of RORα and RORγt can reverse the inhibitory effect of compound 5D on Th17 differentiation

So far, our data indicate that inhibition of Ca^{2+} signaling suppresses Th17 differentiation and expansion. However, it is not clear whether this suppression is caused by indirect effect of blocking cell proliferation, inducing cell death, or inhibition of specific signaling pathways required for Th17 differentiation. Thus, we examined IL-17A$^+$ populations during different division cycles of CFSE-labeled cells incubated with compound 5D. Consistent with the important role of Ca^{2+} signaling in T cell proliferation after stimulation, treatment with compound 5D suppressed proliferation (Fig. 3A). However, even within the same division cycle, compound 5D–treated cells showed much lower IL-17 production. In addition, we did not observe any significant difference in cell death in the absence or presence of compound 5D under Th17-polarizing conditions (data not shown). These results suggest that suppression of Th17 differentiation by compound 5D is derived primarily from a direct block of signaling pathways, independent of cell proliferation or cell death.

Because treatment with compound 5D specifically reduced expression of RORα and RORγt in Th17 cells, not other cellular factors (Fig. 2E, Supplemental Fig. 2C), we examined whether overexpression of these transcription factors can override the inhibitory effect of compound 5D on Th17 differentiation. Moderate expression of RORα or RORγt slightly enhanced IL-17A production in control cells; however, it significantly rescued IL-17A expression in compound 5D–treated cells (Fig. 3B). These results further demonstrated a direct role of CRAC channels in Th17 differentiation by regulating the expression of RORα and RORγt.

Orai1-NFAT-RORα/γt axis plays a crucial role in Th17 differentiation

Previous studies have predicted putative NFAT-binding elements within the RORγt promoter (45, 46). In addition, expression of

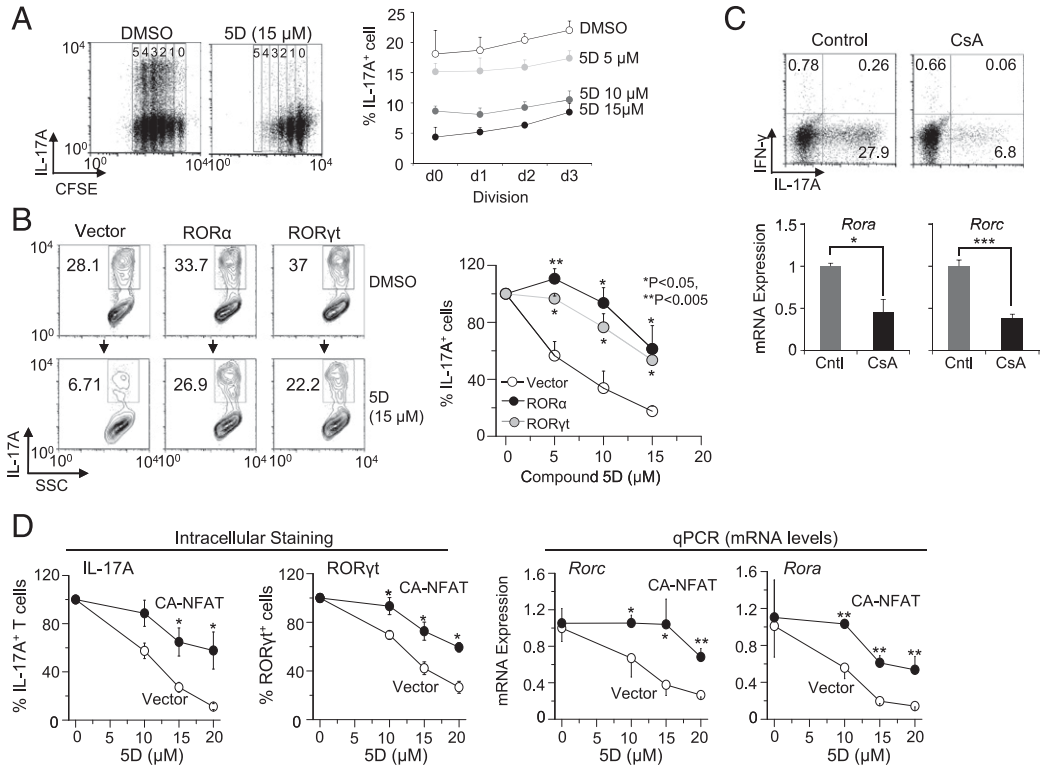

FIGURE 3. Ca^{2+} signaling mediated by Orai1 is important for NFAT-mediated expression of RORα and RORγt in Th17 cells. (**A**) Compound 5D treatment reduces IL-17A production irrespective of blocking proliferation. CFSE-labeled naive cells differentiated under Th17-polarizing conditions with compound 5D were examined for IL-17A production in each division after 3 d of stimulation. Line graph shows average ± SD from three independent experiments. (**B**) Recovery of IL-17A$^+$ population by expression of RORα and RORγt in compound 5D–treated cells. Naive T cells cultured under Th17-polarizing conditions with compound 5D were transduced with retroviruses encoding RORα or RORγt, and examined for IL-17A production on day 4. Line graph on the right shows mean ± SEM of IL-17A$^+$ population from four independent experiments. (**C**) Cyclosporin A (CsA) treatment suppresses expression of IL-17A, RORα, and RORγt. Naive T cells were cultured under Th17-polarizing conditions with 5 nM CsA for 4 d, washed, restimulated with PMA and ionomycin, and examined for production of IL-17A (*top panels*) and mRNA levels of RORα or RORγt (*bottom panels*). Intracellular staining data are representative of three independent experiments. Transcript analysis shows mean ± SD. (**D**) Expression of CA-NFAT rescues compound 5D–mediated inhibition of Th17 differentiation. Naive T cells cultured under Th17-polarizing conditions with different concentrations of compound 5D were transduced with retroviruses encoding CA-NFAT, and examined for IL-17A production and RORγt expression on day 4 using intracellular staining (*left two panels*). The same cells were also used for mRNA expression analysis of RORα or RORγt (*right two panels*). *$p < 0.05$, **$p < 0.005$, ***$p < 0.0005$. Cntl, Control.

a constitutively active NFATc2 mutant influenced expression of RORγt during early stages of Th17 differentiation (47). Because the NFAT family of transcription factors is directly activated by SOCE, we examined their role in regulating expression of RORα and RORγt. Naive T cells were stimulated and cultured under Th17-polarizing conditions in the presence of cyclosporine A (CsA), a calcineurin blocker that also inhibits nuclear translocation of NFAT. Blocking calcineurin activity during Th17 differentiation severely reduced IL-17A$^+$ population, consistent with previous observations (Fig. 3C) (48). In addition, both mRNA levels of RORγt and RORα were reduced in the presence of CsA. These results suggested an important role for Ca^{2+}-NFAT signaling pathway in regulating RORα and RORγt expression. We next examined whether constitutive active NFAT (CA-NFAT) could rescue compound 5D treatment–induced defect in RORα and RORγt expression. As shown in Fig. 3D, exogenous expression of CA-NFAT in compound 5D–treated cells during differentiation resulted in a strong recovery of IL-17A$^+$ population, as well as expression of RORα and RORγt.

To examine a direct role of NFAT in expression of RORα and RORγt, we performed ChIP experiments from naive T cells stimulated and cultured under Th17-polarizing conditions with and without compound 5D. These experiments demonstrated a direct recruitment of NFATc2, the predominant NFAT family member in naive T cells (49), on the promoters of RORγt and RORα under Th17-polarizing conditions, which was markedly reduced in compound 5D–treated cells (Fig. 4A, *left two panels*). We further examined the effect of compound 5D treatment on the chromatin structure of the RORγt and RORα promoters in naive and Th17-polarized CD4$^+$ T cells. We measured acetylation of histone 3 at lysine-9 or lysine-14 residues (H3K9/K14Ac), an indication of active transcription site and open chromatin structure, at the promoter regions of RORγt and RORα. These studies demonstrated a severe reduction in H3K9/14 acetylation at the promoter regions of RORγt and RORα in compound 5D–treated T cells (Fig. 4A, *right two panels*). Together, these results demonstrated an important role for Orai-Ca^{2+}-NFAT pathway in the transcription of RORγt and RORα, and thereby Th17 differentiation. Correspondingly, NFAT recruitment and acetylation of H3K9 and H3K14 at the conserved noncoding sequence 2 and the promoter region of IL-17A were also dramatically reduced in compound 5D–treated cells cultured under Th17-polarizing conditions (Fig. 4B). To examine the effect of blocking NFAT activity on Th1 differentiation, we performed ChIP experiments from naive T cells stimulated and cultured under Th1-polarizing conditions. NFAT recruitment and histone acetylation at the promoter regions of T-bet and IFN-γ were less influenced by treatment with compound 5D (Fig. 4C). These results suggest that a higher sensitivity of Th17 differentiation to compound 5D is at least partly caused by a strong dependence of promoters and enhancers of RORα, RORγt, and IL-17 on the Ca^{2+}-NFAT signaling pathway.

Orai1-deficient T cells recapitulate defects in Th17 differentiation observed in compound 5D–treated cells

To confirm whether compound 5D specifically blocked Orai1 activity, we examined Th17 differentiation of CD4$^+$ T cells isolated from Orai1$^{-/-}$ mice (13). Similar to compound 5D–treated cells,

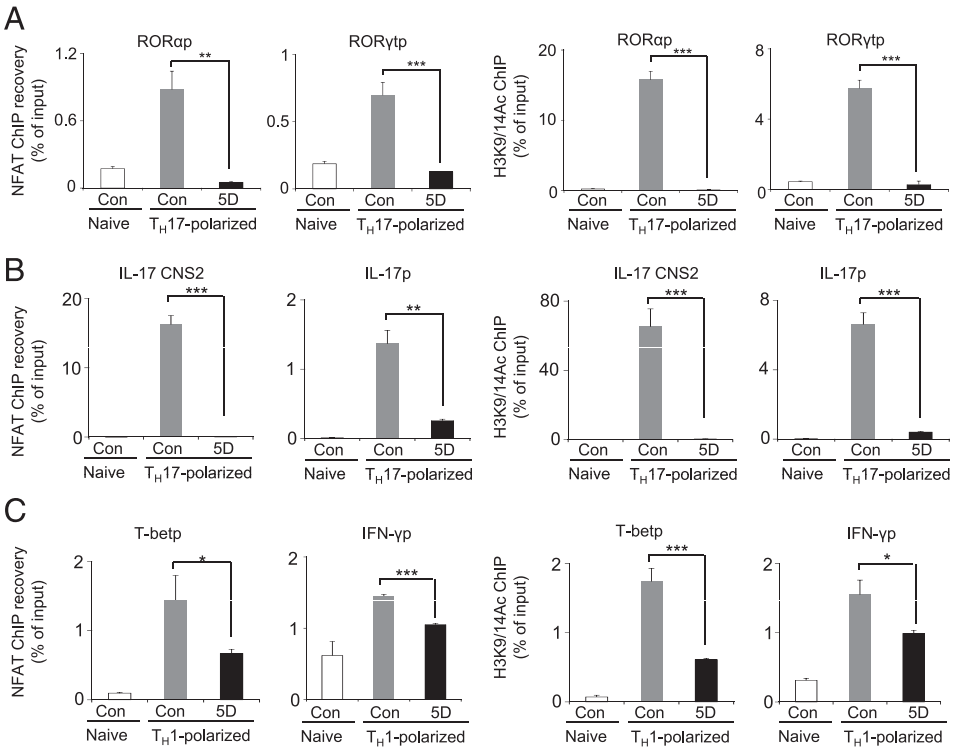

FIGURE 4. Ca^{2+} signaling mediated by Orai1 is important for NFAT-mediated expression of RORα and RORγt in Th17 cells. (**A**) ChIP-PCR analysis of NFAT recruitment and acetylation of histone H3K9/14 at the promoters of RORα or RORγt. Real-time PCR quantification of RORα and RORγt promoter (RORαp and RORγtp) sequences after ChIP with Ab to NFATc2 (*left two panels*), and acetylated H3K9 and H3K14 (H3K9/14Ac, *right two panels*) in DMSO and compound 5D–treated cells after stimulation with anti-CD3 and anti-CD28 Abs for 16 h under Th17-polarizing conditions. Data were normalized to the mean ChIP recovery of all experiments. (**B**) ChIP-PCR analysis of NFAT recruitment and acetylation of histone H3K9/14 at the promoter (IL-17p) and enhancer (conserved noncoding sequence 2 [CNS2]) of IL-17A in the presence and absence of compound 5D. Naive T cells were stimulated with anti-CD3 and anti-CD28 Abs for 16 h under Th17-polarizing conditions. (**C**) ChIP-PCR analysis of NFAT recruitment and acetylation of histone H3K9/14 at the promoters of T-bet and INF-γ. Quantitative RT-PCR analyses after ChIP with Ab to NFATc2 (*left two panels*) and acetylated H3K9 and H3K14 (H3K9/14Ac, *right two panels*) in DMSO and compound 5D–treated cells after stimulation with anti-CD3 and anti-CD28 Abs for 16 h under Th1-polarizing conditions. $*p < 0.05$, $**p < 0.005$, $***p < 0.0005$.

Orai1$^{-/-}$ T cells cultured under Th17-polarizing conditions showed drastically decreased expression levels of IL-17, RORα, and RORγt (Fig. 5A, 5B). Transcript analysis showed a pronounced reduction in expression levels of cytokines and receptors including IL-17A, IL-17F, IL-22, and IL-23R in Orai1$^{-/-}$ T cells (Fig. 5C). To investigate whether NFAT can recover the defective Th17 differentiation observed in Orai1$^{-/-}$ T cells, we transduced these cells with CA-NFAT. Expression of CA-NFAT almost completely recovered expression of RORα and RORγt, and moderately rescued IL-17A expression in Orai1$^{-/-}$ cells (Fig. 5D). Furthermore, the recruitment of NFAT to the promoters of RORα and RORγt was severely decreased in Orai1$^{-/-}$ T cells cultured under Th17-polarized conditions, similar to results obtained from compound 5D–treated cells (Fig. 5E). These results, together with the rescue experiments from compound 5D–treated cells, strongly suggested that expression of RORα and RORγt is regulated by the Orai-Ca^{2+}-NFAT signaling pathway.

Amelioration of EAE by CRAC channel inhibition

To examine the effects of CRAC channel inhibition in vivo, we used a mouse model of inflammation, EAE, where the pathogenic function of inflammatory T cells is extensively studied. Compound 5D treatment greatly ameliorated EAE in vivo by delaying the onset of symptoms, reducing the clinical score, and decreasing T cell infiltration into the CNS (Fig. 6A); however, it also influenced the survival of mice when injected at 2 mg/kg every alternate day (data not shown). A careful structural analysis revealed possible in vivo toxicity because of the trichloride (-Cl_3) motif present in compound 5D. Thus, various structural analogs of compound 5D lacking this motif were examined for blocking SOCE. This study identified compound 5J-4, which showed a strong block of SOCE in HeLa-O+S cells, as well as endogenous SOCE in Th17 cells, comparable with that observed with compound 5D (Fig. 6B, 6C). Moreover, in vivo injection of 2 mg/kg compound 5J-4 every alternate day did not cause any lethality in mice (Supplemental Fig. 3A). Injection of compound 5J-4 into $MOG_{35–55}$ peptide–immunized mice dramatically reduced the symptoms and delayed the onset of EAE, demonstrating its protective effects on autoimmunity (Fig. 6D, Supplemental Fig. 3B). Consistent with the clinical score, infiltrated mononuclear cell numbers into the CNS were reduced and, in particular, the infiltrated CD4$^+$ population was significantly decreased (Fig. 6E, Supplemental Fig. 3C). Next, we examined cytokine production by the mononuclear cells isolated from the draining lymph nodes and CNS of compound 5J-4–treated animals. In support of our in vitro and ex vivo data, we observed a predominant reduction in IL-17A$^+$ population, whereas that of IFN-γ$^+$ cells was not significantly reduced (Fig. 7A). Although a majority of compound 5J-4–treated mice (~70%) exhibited this phenotype, there was a population of ~30% animals that showed a strong resistance to EAE and correspondingly reduction in both IFN-γ$^+$ and IL-17A$^+$ populations of cells (data not shown). This phenotype could be because of variation in immunization efficacy or response of individual animals. To examine whether reduced infiltration of T cells in the CNS was caused by a decrease in T cell differentiation, we analyzed the function of inflammatory T cells from the draining lymph nodes of control and 5J-4–injected mice. The mRNA levels of RORα and RORγt were dramatically reduced, whereas those of T-bet and Foxp3 were not significantly affected (Supplemental Fig. 3D). These results suggest that, consistent with in vitro

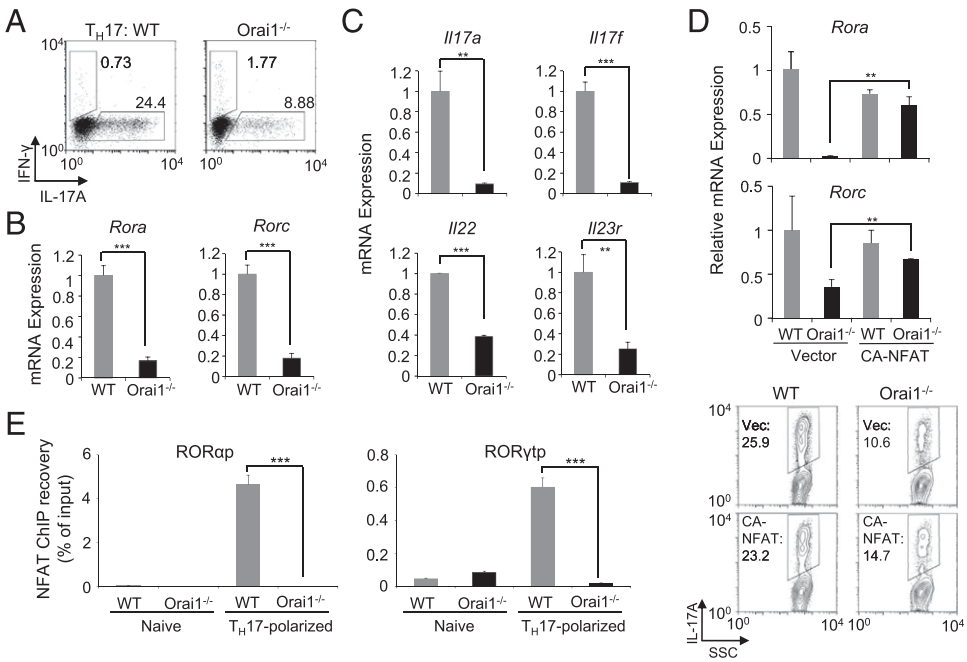

FIGURE 5. Orai1$^{-/-}$ T cells show a defect in Th17 differentiation similar to that observed in compound 5D–treated cells. (**A**) Orai1$^{-/-}$ T cells show a defect in IL-17 production. Naive CD4$^+$ T cells were stimulated and cultured under Th17-polarizing conditions, restimulated with PMA and ionomycin after 4 d, and examined for IL-17A expression. (**B**) mRNA expression analyses of RORα and RORγt in control and Orai1$^{-/-}$ T cells after stimulation with anti-CD3 and anti-CD28 Abs under Th17-polarizing conditions for 4 d. (**C**) mRNA expression analyses in Orai1$^{-/-}$ T cells cultured under Th17-polarizing conditions. WT and Orai1$^{-/-}$ naive T cells cultured under Th17-polarizing conditions for 4 d were stimulated with PMA and ionomycin, and analyzed for expression of indicated genes. (**D**) Expression of CA-NFAT partially rescues Th17 differentiation defect in Orai1$^{-/-}$ T cells. WT and Orai1$^{-/-}$ naive T cells differentiated under Th17-polarizing conditions were transduced with retroviruses encoding CA-NFAT, and examined for mRNA expression of RORα or RORγt (*top panels*) and IL-17A production (*lower panels*). (**E**) ChIP-PCR analysis of NFAT recruitment onto the promoters of RORα or RORγt. Quantitative RT-PCR analysis of RORα and RORγt promoter (RORαp and RORγtp) sequences after ChIP recovery with Ab to NFATc2 in control and Orai1$^{-/-}$ T cells left unstimulated (naive) or stimulated with anti-CD3 and anti-CD28 Abs for 16 h under Th17-polarizing conditions. Data were normalized to the mean ChIP recovery of all experiments. $^{**}p < 0.005$, $^{***}p < 0.0005$.

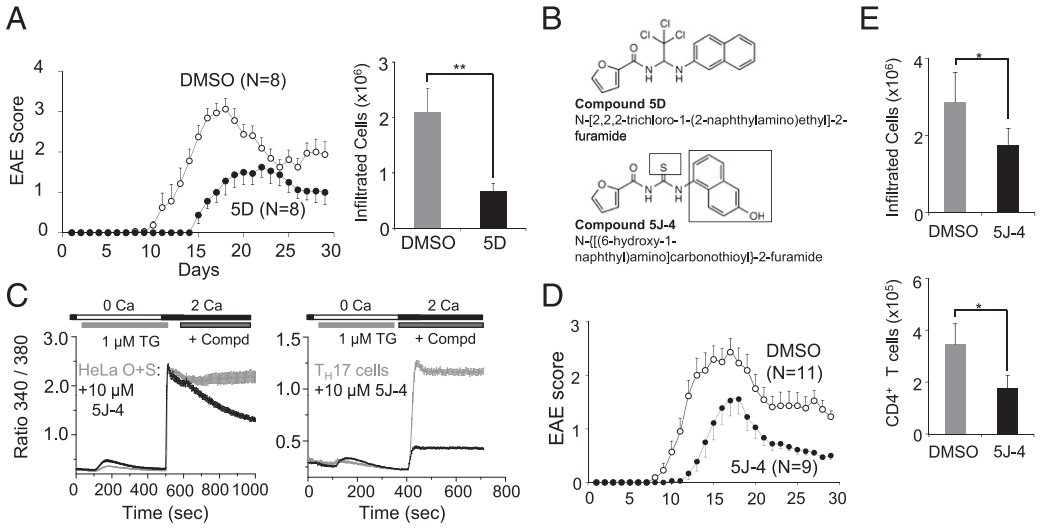

FIGURE 6. Compound 5D and 5J-4 ameliorate Th17-mediated autoimmune disease. (**A**) EAE disease course in C57BL/6 mice injected i.p. with either carrier alone or compound 5D (1 mg/kg) every alternate day starting from day −1. At day 0, disease was induced with injection of $MOG_{35–55}$/CFA. The graph shows average ± SEM and is representative of 3 experiments with 8–10 animals in each experiment. (**B**) Chemical structures of compound 5D and its analog, compound 5J-4. (**C**) Measurement of block of SOCE by compound 5J-4 in HeLa-OSN cells (*left panel*) or primary Th17 cells (*right panel*). In all, the graphs data represent average ± SEM from 25–35 different cells. (**D**) Compound 5J-4 ameliorates symptoms of EAE in vivo. EAE disease course in mice injected i.p. with either DMSO or compound 5J-4 (2 mg/kg) every alternate day starting from day 0 after disease induction with $MOG_{35–55}$/CFA. The graph shows average ± SEM from 1 of 3 independent repeats of the experiments with 10–20 mice per trial. (**E**) Compound 5J-4 reduces infiltration of mononuclear cells into the CNS when administered in vivo. Mononuclear cells purified from the CNS of control and compound 5J-4–treated mice were counted (*top panel*) or examined for numbers of $CD4^+$ T cells (*bottom panel*) ($n = 4$). $^*p < 0.05$, $^{**}p < 0.005$.

observations, injection of compound 5J-4 interfered with T cell differentiation after immunization that led to reduced numbers of inflammatory T cells into the CNS of EAE-induced mice. To examine whether CRAC channel function is important for sustained expression of IL-17A even in human $CD4^+$ T cells, we stimulated human PBMCs and cultured them under Th17-expanding conditions by inclusion of IL-1β, IL-23, and IL-2. In the control cells, we observed expression of both IFN-γ and IL-17A from $CD4^+$ T cells (Fig. 7B, left plot). Importantly, blocking of CRAC channels led to >50% reduction in $IL\text{-}17A^+$ population with little

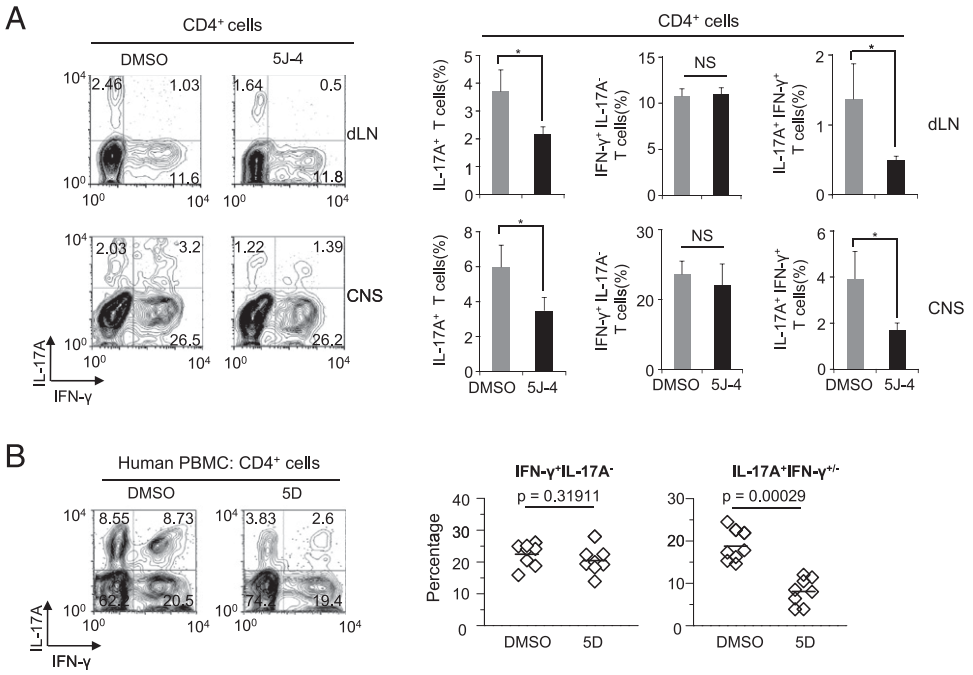

FIGURE 7. Treatment with CRAC channel blockers reduces differentiation and expansion of Th17 cells. (**A**) Compound 5J-4 treatment preferentially decreases Th17 differentiation in vivo. Expression levels of IFN-γ and IL-17A were measured in cells isolated from the draining lymph nodes (dLN) and CNS of DMSO and compound 5J-4–treated mice after 14 d of immunization with $MOG_{35–55}$ peptide/CFA. Cells were stimulated with PMA and ionomycin, and stained for CD4, IFN-γ, and IL-17A. Bar graphs on the right show average ± standard deviation of mean of indicated population of T cells from four mice. (**B**) Suppression of expansion and maintenance of predifferentiated human Th17 cells by inhibition of CRAC channel activity. Human PBMCs were harvested, stimulated with anti-CD3 and anti-CD28 Abs, and cultured with IL-1β and IL-23 in the presence of DMSO or 20 μM compound 5D. Cells were restimulated with PMA and ionomycin at day 6, and examined for IL-17A and IFN-γ production. The graph shows results from eight donors. $^*p < 0.05$.

effect on IFN-γ^+ cells (Fig. 7B, graphs). These results demonstrate that CRAC channels have an important role in maintenance and expansion of human Th17 population, similar to murine Th17 cells.

Discussion

In this study, we identified a novel class of CRAC channel blockers using high-throughput chemical library screen and asked how inhibition of Ca^{2+} signaling during TCR stimulation influenced differentiation and effector functions of T cells in vitro and in vivo. Using a combination of NFAT translocation as readout and a cell line harboring amplified CRAC currents, we identified a novel class of immunomodulators, compound 5, and its analogs. A more potent analog of the lead compound, compound 5D, blocked CRAC currents generated by WT Orai1 and a constitutively active mutant of Orai1 without affecting Orai1 and STIM1 translocation, indicating that the blocking mechanism directly involves the pore-forming subunit, Orai1. Further studies of CRAC current inhibition showed block by extracellular, but not intracellular, application of compound 5D, suggesting that the binding site is accessible only from the extracellular face of Orai1. Comprehensive mutational analysis of all the residues with possible exposure to the extracellular milieu identified the putative channel gate V102 to be important for the blocking activity of compound 5D. Furthermore, compound 5D blocked SOCE mediated by all the Orai proteins; however, that by TrpC1 remained unaffected, indicating a specific block of CRAC channel activity (Fig. 1, Supplemental Fig. 1).

After differentiation, effector T cells become activated by secondary engagement of TCR to produce cytokines in a Ca^{2+}-NFAT signaling–dependent manner. Thus, blocking CRAC channel activity was expected to reduce cytokine production upon secondary engagement of TCR in effector T cells (Fig. 2A–C). Interestingly, blocking CRAC channels also had an inhibitory effect on naive T cell differentiation upon first engagement of TCR, with preferential inhibition of Th17 differentiation, and, to a lesser extent, Th1 and Th2 differentiation (Fig. 2D, 2E). Previously, we showed that Orai1-deficient T cells cultured under Th1- and Th2-polarizing conditions showed a pronounced reduction in expression of IFN-γ and IL-4, respectively (13). Although reduction in IFN-γ levels is similar in both compound 5D–treated and Orai1-deficient Th1 cells, that of IL-4 is less pronounced in compound 5D–treated Th2 cells. This difference in Th2 cells may be because of lack of Orai1 for the entire duration of differentiation, as well as restimulation for cytokine production in Orai1-deficient T cells. Although it was previously shown that the conserved noncoding sequence 1 region in the Foxp3 promoter contains NFAT-binding element (50), inhibition of CRAC channel activity did not significantly influence development of inducible Tregs (Supplemental Fig. 2A). We do not know the exact reason for this discrepancy, but it is possible that the requirement for intracellular Ca^{2+} levels in Treg development is low; thus, the residual Ca^{2+} levels after blocker treatment may be sufficient for induction of Foxp3. This idea is further supported by the results from double knockout of STIM1 and STIM2 showing reduced levels of Foxp3$^+$ Tregs, whereas individual knockouts did not affect Treg development (15).

Th17 cells showed higher sensitivity to decreased levels of $[Ca^{2+}]_i$. At the present stage, the exact molecular mechanism behind this is not very clear. Previous studies have shown that upon Ag stimulation, Th17 cells exhibit a distinct Ca^{2+} profile from Th1 and Th2 cells (36). Th17 cells showed increased $[Ca^{2+}]_i$ with robust oscillations and correspondingly increased nuclear accumulation of NFAT for longer times than Th2 cells (36). These data suggest that SOCE may play a more important role in differentiation of Th17 cells than that of Th1 and Th2 cells. Specific usage of Ca^{2+} channels in different effector T cells was also observed in the studies of L-type voltage-gated Ca^{2+} (Ca_V1) channels. Administration of Ca_V1 blocker reduced Th2 response, but not Th1 response, in vitro and in vivo (51). Our data with CRAC channel blockers strongly support all these observations. First, moderate concentration of compound 5D (1 μM) reduced SOCE by >85% in Th17 cells, whereas the block was <50% in Th1 cells (Fig. 2A). Because Orai proteins are known to heteromultimerize, the subunit stoichiometry and/or expression levels of Orai family members may contribute to the higher reduction in SOCE in Th17 cells. Second, it is possible that Th17 differentiation may exhibit higher dependence on the Orai-NFAT pathway. Previous studies had predicted putative NFAT-binding elements on the RORγt promoter (45, 46) and an involvement of NFAT in IL-17, IL-21, and IL-22 production in Th17 cells (48, 52). We also observed recruitment of NFAT onto the promoters and enhancers of RORα, RORγt, and IL-17A, which was reduced in compound 5D–treated or Orai1-deficient T cells (Figs. 4, 5). Consistent with these studies, blocking NFAT translocation using CsA reduced expression of RORα and RORγt in T cells cultured under Th17-polarizing conditions (Fig. 3C). Conversely, expression of CA-NFAT showed a strong rescue of the expression of RORα and RORγt in both compound 5D–treated and Orai1-deficient Th17 cells (Figs. 3, 5). Another unexplored possibility is, in addition to regulating NFAT activity, Ca^{2+} signaling may play an important role in activating other signaling pathway(s) important for Th17 differentiation. Signaling pathways at the early stage of T cell differentiation such as TCR stimulation in conjugation with Th17-polarizing cytokines may be involved in preconditioning of epigenetic status of chromatin for further lineage-specific differentiation, and Ca^{2+} signaling triggered by TCR stimulation can be a part of these early TCR stimulation–triggered signaling pathways. Future experiments examining epigenetic modifications in WT and Orai1-deficient Th17 cells can help in uncovering this hypothesis.

Notably, the blocking effect of compound 5D had selective inhibitory effects on the expression levels of RORα and RORγt, not on other transcription factors important for Th17 differentiation (Fig. 2E, Supplemental Fig. 2C). Exogenous expression of RORα and RORγt could significantly reverse the inhibitory effect of compound 5D on IL-17A production (Fig. 3B). In addition, the inhibitory effect of CRAC channel blocker on IL-17 production did not show a strong correlation with the cell division rate (Fig. 3A). Therefore, contrary to the general concept that blocking Ca^{2+} signaling triggered by TCR stimulation leads to inhibition of T cell proliferation followed by suppression of T cell differentiation, inhibition of Orai1 activity suppresses selective signaling pathways important for Th17 differentiation. Previous studies of transcriptional regulation of RORα and RORγt promoters have suggested an important role for STAT3 and c-Rel transcription factors. Durant et al. (53) used genome-wide ChIP and parallel sequencing (ChIP-seq) experiments from WT and STAT3-deficient T cells cultured under Th17-polarizing condition and identified recruitment of STAT3 to both RORα and RORγt promoters. Consequently, expression levels of RORα and RORγt were significantly reduced in STAT3-deficient T cells. More recently, using ChIP and luciferase reporter assays, Ruan et al. (46) have shown a direct regulation of RORγt expression by c-Rel. Furthermore, the authors also observed reduced expression of RORα transcripts in c-Rel–deficient T cells. Our studies now add another transcription factor, NFAT, as a direct regulator of both RORα and RORγt expression. Contrary to Th1 and Th2 cells, Th17 cells have intrinsic instability as demonstrated by extended in vitro culture or adoptive transfer (54). In addition to differentiation, maintenance of IL-17 production needs continued expression of RORγt controlled

by IL-6, IL-21, and IL-23 (55, 56). Orai1-mediated Ca^{2+} signaling is not only required for differentiation but also is important for maintenance and expansion of Th17 cells. When compound 5D was included during the maintenance and expansion of predifferentiated Th17 cells ex vivo, a strong suppression of IL-17 production was observed (Fig. 2F). These results suggest that in addition to STAT3-inducing cytokines, high levels of Ca^{2+} signaling triggered by TCR stimulation are required for stable maintenance of Th17 cells to reduce plasticity.

Consistent with the results from in vitro experiments, Orai1 blockers had a potent anti-inflammatory effect in vivo. Compound 5D or 5J-4 treatment blocked infiltration of T cells into the CNS and reduced IL-17–producing cells, as well as expression of RORα and RORγt (Figs. 6, 7). The expression levels of Foxp3 were not dramatically changed in either in vitro or in vivo experimental settings (Supplemental Fig. 2A, 3D). These observations lead into an interesting hypothesis that highly inflammatory T cells such as Th17 require high Ca^{2+} levels for their generation and maintenance, whereas the Ca^{2+} requirement for other effector and Tregs is moderate and low, respectively.

Recent screening studies have identified various small molecules that block the function of inflammatory T cells. Digoxin and its derivatives were identified from a small-molecule library screen using transcriptional activity of RORγt as readout (57). In addition, a synthetic ligand, SR1001, was also identified as a blocker for the transcriptional activities of RORγt and RORα (58). Both these small-molecule blockers showed protective effects on EAE. The molecular mechanism of the anti-inflammatory effect of another small molecule halofuginone was recently elucidated. Instead of acting on orphan receptors directly, halofuginone was shown to activate the amino acid starvation response pathway (59). Halofuginone influenced the functions of Th1, Th2, and Th17 cells at high concentrations; however, it selectively suppressed cytokine production by Th17 cells at low concentrations and alleviated the symptoms of EAE when administered in vivo. Although the outcomes of these small molecules are similar (e.g., anti-inflammatory effects), their working mechanisms are distinct from each other. CRAC channel blockers can be considered as general immunosuppressants taking into account their broad role in various immune cells. Earlier, a pyrazole derivative and RO2959 were identified as CRAC channel blockers and were shown to have high potency to suppress T cell function in vitro (60–62). However, our results suggest that compound 5D and its derivatives can have a stronger blocking effect on inflammatory Th17 cells than other T cell subsets, suggesting their potential usage in selective T cell subsets.

Human patients with nonfunctional CRAC channels suffer from fatal SCID, which can be rescued by bone marrow transplantation (63). These studies suggest a predominant role for CRAC channels in immune cells. Hence blockers of CRAC channels are likely to have fewer side effects than widely used immunosuppressive drugs such as cyclosporin A and tacrolimus that block calcineurin activity. Our studies reveal that small-molecule blockers of CRAC channels can provide a molecular probe to examine the role of Ca^{2+} signaling in the immune system, and potentially lead to novel and improved therapeutic approaches to suppress hypersensitive immune responses by blocking cytokine production in the short term, and reducing differentiation and survival/expansion of inflammatory T cells in the long term.

Acknowledgments

We thank staff members of Molecular Screening Shared Resources and University of California Los Angeles Jonsson Comprehensive Cancer Center Flow Cytometry Core Facility for technical help. We thank Drs. Ernest Wright and Kenneth Philipson for advice on this project.

Disclosures

The authors have no financial conflicts of interest.

References

1. Lewis, R. S. 2011. Store-operated calcium channels: new perspectives on mechanism and function. *Cold Spring Harb. Perspect. Biol.* 3: a003970.
2. Srikanth, S., and Y. Gwack. 2013. Orai1-NFAT signalling pathway triggered by T cell receptor stimulation. *Mol. Cells* 35: 182–194.
3. Zhang, S. L., A. V. Yeromin, X. H. Zhang, Y. Yu, O. Safrina, A. Penna, J. Roos, K. A. Stauderman, and M. D. Cahalan. 2006. Genome-wide RNAi screen of Ca(2+) influx identifies genes that regulate Ca(2+) release-activated Ca(2+) channel activity. *Proc. Natl. Acad. Sci. USA* 103: 9357–9362.
4. Vig, M., C. Peinelt, A. Beck, D. L. Koomoa, D. Rabah, M. Koblan-Huberson, S. Kraft, H. Turner, A. Fleig, R. Penner, and J. P. Kinet. 2006. CRACM1 is a plasma membrane protein essential for store-operated Ca2+ entry. *Science* 312: 1220–1223.
5. Feske, S., Y. Gwack, M. Prakriya, S. Srikanth, S. H. Puppel, B. Tanasa, P. G. Hogan, R. S. Lewis, M. Daly, and A. Rao. 2006. A mutation in Orai1 causes immune deficiency by abrogating CRAC channel function. *Nature* 441: 179–185.
6. Gwack, Y., S. Srikanth, S. Feske, F. Cruz-Guilloty, M. Oh-hora, D. S. Neems, P. G. Hogan, and A. Rao. 2007. Biochemical and functional characterization of Orai proteins. *J. Biol. Chem.* 282: 16232–16243.
7. Liou, J., M. L. Kim, W. D. Heo, J. T. Jones, J. W. Myers, J. E. Ferrell, Jr., and T. Meyer. 2005. STIM is a Ca2+ sensor essential for Ca2+-store-depletion-triggered Ca2+ influx. *Curr. Biol.* 15: 1235–1241.
8. Roos, J., P. J. DiGregorio, A. V. Yeromin, K. Ohlsen, M. Lioudyno, S. Zhang, O. Safrina, J. A. Kozak, S. L. Wagner, M. D. Cahalan, et al. 2005. STIM1, an essential and conserved component of store-operated Ca2+ channel function. *J. Cell Biol.* 169: 435–445.
9. Zhang, S. L., Y. Yu, J. Roos, J. A. Kozak, T. J. Deerinck, M. H. Ellisman, K. A. Stauderman, and M. D. Cahalan. 2005. STIM1 is a Ca2+ sensor that activates CRAC channels and migrates from the Ca2+ store to the plasma membrane. *Nature* 437: 902–905.
10. Liou, J., M. Fivaz, T. Inoue, and T. Meyer. 2007. Live-cell imaging reveals sequential oligomerization and local plasma membrane targeting of stromal interaction molecule 1 after Ca2+ store depletion. *Proc. Natl. Acad. Sci. USA* 104: 9301–9306.
11. Putney, J. W., Jr. 1986. A model for receptor-regulated calcium entry. *Cell Calcium* 7: 1–12.
12. Picard, C., C. A. McCarl, A. Papolos, S. Khalil, K. Lüthy, C. Hivroz, F. LeDeist, F. Rieux-Laucat, G. Rechavi, A. Rao, et al. 2009. STIM1 mutation associated with a syndrome of immunodeficiency and autoimmunity. *N. Engl. J. Med.* 360: 1971–1980.
13. Gwack, Y., S. Srikanth, M. Oh-Hora, P. G. Hogan, E. D. Lamperti, M. Yamashita, C. Gelinas, D. S. Neems, Y. Sasaki, S. Feske, et al. 2008. Hair loss and defective T- and B-cell function in mice lacking ORAI1. *Mol. Cell. Biol.* 28: 5209–5222.
14. Matsumoto, M., Y. Fujii, A. Baba, M. Hikida, T. Kurosaki, and Y. Baba. 2011. The calcium sensors STIM1 and STIM2 control B cell regulatory function through interleukin-10 production. *Immunity* 34: 703–714.
15. Oh-Hora, M., M. Yamashita, P. G. Hogan, S. Sharma, E. Lamperti, W. Chung, M. Prakriya, S. Feske, and A. Rao. 2008. Dual functions for the endoplasmic reticulum calcium sensors STIM1 and STIM2 in T cell activation and tolerance. *Nat. Immunol.* 9: 432–443.
16. Schuhmann, M. K., D. Stegner, A. Berna-Erro, S. Bittner, A. Braun, C. Kleinschnitz, G. Stoll, H. Wiendl, S. G. Meuth, and B. Nieswandt. 2010. Stromal interaction molecules 1 and 2 are key regulators of autoreactive T cell activation in murine autoimmune central nervous system inflammation. *J. Immunol.* 184: 1536–1542.
17. Vig, M., W. I. DeHaven, G. S. Bird, J. M. Billingsley, H. Wang, P. E. Rao, A. B. Hutchings, M. H. Jouvin, J. W. Putney, and J. P. Kinet. 2008. Defective mast cell effector functions in mice lacking the CRACM1 pore subunit of store-operated calcium release-activated calcium channels. *Nat. Immunol.* 9: 89–96.
18. Bettelli, E., Y. Carrier, W. Gao, T. Korn, T. B. Strom, M. Oukka, H. L. Weiner, and V. K. Kuchroo. 2006. Reciprocal developmental pathways for the generation of pathogenic effector TH17 and regulatory T cells. *Nature* 441: 235–238.
19. Veldhoen, M., R. J. Hocking, C. J. Atkins, R. M. Locksley, and B. Stockinger. 2006. TGFbeta in the context of an inflammatory cytokine milieu supports de novo differentiation of IL-17-producing T cells. *Immunity* 24: 179–189.
20. Korn, T., E. Bettelli, M. Oukka, and V. K. Kuchroo. 2009. IL-17 and Th17 cells. *Annu. Rev. Immunol.* 27: 485–517.
21. Zhou, L., and D. R. Littman. 2009. Transcriptional regulatory networks in Th17 cell differentiation. *Curr. Opin. Immunol.* 21: 146–152.
22. O'Shea, J. J., R. Lahesmaa, G. Vahedi, A. Laurence, and Y. Kanno. 2011. Genomic views of STAT function in CD4+ T helper cell differentiation. *Nat. Rev. Immunol.* 11: 239–250.
23. Dong, C. 2008. TH17 cells in development: an updated view of their molecular identity and genetic programming. *Nat. Rev. Immunol.* 8: 337–348.
24. Yang, X. O., B. P. Pappu, R. Nurieva, A. Akimzhanov, H. S. Kang, Y. Chung, L. Ma, B. Shah, A. D. Panopoulos, K. S. Schluns, et al. 2008. T helper 17 lineage differentiation is programmed by orphan nuclear receptors ROR alpha and ROR gamma. *Immunity* 28: 29–39.
25. Constant, S. L., and K. Bottomly. 1997. Induction of Th1 and Th2 CD4+ T cell responses: the alternative approaches. *Annu. Rev. Immunol.* 15: 297–322.

26. Gwack, Y., S. Sharma, J. Nardone, B. Tanasa, A. Iuga, S. Srikanth, H. Okamura, D. Bolton, S. Feske, P. G. Hogan, and A. Rao. 2006. A genome-wide Drosophila RNAi screen identifies DYRK-family kinases as regulators of NFAT. *Nature* 441: 646–650.
27. Srikanth, S., H. J. Jung, K. D. Kim, P. Souda, J. Whitelegge, and Y. Gwack. 2010. A novel EF-hand protein, CRACR2A, is a cytosolic Ca2+ sensor that stabilizes CRAC channels in T cells. *Nat. Cell Biol.* 12: 436–446.
28. Srikanth, S., M. Jew, K. D. Kim, M. K. Yee, J. Abramson, and Y. Gwack. 2012. Junctate is a Ca2+-sensing structural component of Orai1 and stromal interaction molecule 1 (STIM1). *Proc. Natl. Acad. Sci. USA* 109: 8682–8687.
29. Srikanth, S., M. K. Yee, Y. Gwack, and B. Ribalet. 2011. The third transmembrane segment of orai1 protein modulates Ca2+ release-activated Ca2+ (CRAC) channel gating and permeation properties. *J. Biol. Chem.* 286: 35318–35328.
30. McNally, B. A., M. Yamashita, A. Engh, and M. Prakriya. 2009. Structural determinants of ion permeation in CRAC channels. *Proc. Natl. Acad. Sci. USA* 106: 22516–22521.
31. Zhou, Y., S. Ramachandran, M. Oh-Hora, A. Rao, and P. G. Hogan. 2010. Pore architecture of the ORAI1 store-operated calcium channel. *Proc. Natl. Acad. Sci. USA* 107: 4896–4901.
32. McNally, B. A., A. Somasundaram, M. Yamashita, and M. Prakriya. 2012. Gated regulation of CRAC channel ion selectivity by STIM1. *Nature* 482: 241–245.
33. Kim, K. D., S. Srikanth, M. K. Yee, D. C. Mock, G. W. Lawson, and Y. Gwack. 2011. ORAI1 deficiency impairs activated T cell death and enhances T cell survival. *J. Immunol.* 187: 3620–3630.
34. DeHaven, W. I., J. T. Smyth, R. R. Boyles, and J. W. Putney, Jr. 2007. Calcium inhibition and calcium potentiation of Orai1, Orai2, and Orai3 calcium release-activated calcium channels. *J. Biol. Chem.* 282: 17548–17556.
35. Lis, A., C. Peinelt, A. Beck, S. Parvez, M. Monteilh-Zoller, A. Fleig, and R. Penner. 2007. CRACM1, CRACM2, and CRACM3 are store-operated Ca2+ channels with distinct functional properties. *Curr. Biol.* 17: 794–800.
36. Weber, K. S., M. J. Miller, and P. M. Allen. 2008. Th17 cells exhibit a distinct calcium profile from Th1 and Th2 cells and have Th1-like motility and NF-AT nuclear localization. *J. Immunol.* 180: 1442–1450.
37. Serfling, E., A. Avots, S. Klein-Hessling, R. Rudolf, M. Vaeth, and F. Berberich-Siebelt. 2012. NFATc1/αA: The other face of NFAT factors in lymphocytes. *Cell Commun. Signal.* 10: 16.
38. Bauquet, A. T., H. Jin, A. M. Paterson, M. Mitsdoerffer, I. C. Ho, A. H. Sharpe, and V. K. Kuchroo. 2009. The costimulatory molecule ICOS regulates the expression of c-Maf and IL-21 in the development of follicular T helper cells and TH-17 cells. *Nat. Immunol.* 10: 167–175.
39. Brüstle, A., S. Heink, M. Huber, C. Rosenplänter, C. Stadelmann, P. Yu, E. Arpaia, T. W. Mak, T. Kamradt, and M. Lohoff. 2007. The development of inflammatory T(H)-17 cells requires interferon-regulatory factor 4. *Nat. Immunol.* 8: 958–966.
40. Chen, Z., A. Laurence, Y. Kanno, M. Pacher-Zavisin, B. M. Zhu, C. Tato, A. Yoshimura, L. Hennighausen, and J. J. O'Shea. 2006. Selective regulatory function of Socs3 in the formation of IL-17-secreting T cells. *Proc. Natl. Acad. Sci. USA* 103: 8137–8142.
41. Dang, E. V., J. Barbi, H. Y. Yang, D. Jinasena, H. Yu, Y. Zheng, Z. Bordman, J. Fu, Y. Kim, H. R. Yen, et al. 2011. Control of T(H)17/T(reg) balance by hypoxia-inducible factor 1. *Cell* 146: 772–784.
42. Schraml, B. U., K. Hildner, W. Ise, W. L. Lee, W. A. Smith, B. Solomon, G. Sahota, J. Sim, R. Mukasa, S. Cemerski, et al. 2009. The AP-1 transcription factor Batf controls T(H)17 differentiation. *Nature* 460: 405–409.
43. Veldhoen, M., K. Hirota, A. M. Westendorf, J. Buer, L. Dumoutier, J. C. Renauld, and B. Stockinger. 2008. The aryl hydrocarbon receptor links TH17-cell-mediated autoimmunity to environmental toxins. *Nature* 453: 106–109.
44. Zhang, F., G. Meng, and W. Strober. 2008. Interactions among the transcription factors Runx1, RORgammat and Foxp3 regulate the differentiation of interleukin 17-producing T cells. *Nat. Immunol.* 9: 1297–1306.
45. Xi, H., R. Schwartz, I. Engel, C. Murre, and G. J. Kersh. 2006. Interplay between RORgammat, Egr3, and E proteins controls proliferation in response to pre-TCR signals. *Immunity* 24: 813–826.
46. Ruan, Q., V. Kameswaran, Y. Zhang, S. Zheng, J. Sun, J. Wang, J. DeVirgiliis, H. C. Liou, A. A. Beg, and Y. H. Chen. 2011. The Th17 immune response is controlled by the Rel-RORγ-RORγ T transcriptional axis. *J. Exp. Med.* 208: 2321–2333.
47. Ghosh, S., S. B. Koralov, I. Stevanovic, M. S. Sundrud, Y. Sasaki, K. Rajewsky, A. Rao, and M. R. Müller. 2010. Hyperactivation of nuclear factor of activated T cells 1 (NFAT1) in T cells attenuates severity of murine autoimmune encephalomyelitis. *Proc. Natl. Acad. Sci. USA* 107: 15169–15174.
48. Gomez-Rodriguez, J., N. Sahu, R. Handon, T. S. Davidson, S. M. Anderson, M. R. Kirby, A. August, and P. L. Schwartzberg. 2009. Differential expression of interleukin-17A and -17F is coupled to T cell receptor signaling via inducible T cell kinase. *Immunity* 31: 587–597.
49. Macián, F., F. García-Cózar, S. H. Im, H. F. Horton, M. C. Byrne, and A. Rao. 2002. Transcriptional mechanisms underlying lymphocyte tolerance. *Cell* 109: 719–731.
50. Tone, Y., K. Furuuchi, Y. Kojima, M. L. Tykocinski, M. I. Greene, and M. Tone. 2008. Smad3 and NFAT cooperate to induce Foxp3 expression through its enhancer. *Nat. Immunol.* 9: 194–202.
51. Badou, A., M. K. Jha, D. Matza, and R. A. Flavell. 2013. Emerging roles of L-type voltage-gated and other calcium channels in T lymphocytes. *Front. Immunol.* 4: 243.
52. Spolski, R., and W. J. Leonard. 2008. Interleukin-21: basic biology and implications for cancer and autoimmunity. *Annu. Rev. Immunol.* 26: 57–79.
53. Durant, L., W. T. Watford, H. L. Ramos, A. Laurence, G. Vahedi, L. Wei, H. Takahashi, H. W. Sun, Y. Kanno, F. Powrie, and J. J. O'Shea. 2010. Diverse targets of the transcription factor STAT3 contribute to T cell pathogenicity and homeostasis. *Immunity* 32: 605–615.
54. Mukasa, R., A. Balasubramani, Y. K. Lee, S. K. Whitley, B. T. Weaver, Y. Shibata, G. E. Crawford, R. D. Hatton, and C. T. Weaver. 2010. Epigenetic instability of cytokine and transcription factor gene loci underlies plasticity of the T helper 17 cell lineage. *Immunity* 32: 616–627.
55. Kanno, Y., G. Vahedi, K. Hirahara, K. Singleton, and J. J. O'Shea. 2012. Transcriptional and epigenetic control of T helper cell specification: molecular mechanisms underlying commitment and plasticity. *Annu. Rev. Immunol.* 30: 707–731.
56. Wilson, C. B., E. Rowell, and M. Sekimata. 2009. Epigenetic control of T-helper-cell differentiation. *Nat. Rev. Immunol.* 9: 91–105.
57. Huh, J. R., M. W. Leung, P. Huang, D. A. Ryan, M. R. Krout, R. R. Malapaka, J. Chow, N. Manel, M. Ciofani, S. V. Kim, et al. 2011. Digoxin and its derivatives suppress TH17 cell differentiation by antagonizing RORγt activity. *Nature* 472: 486–490.
58. Solt, L. A., N. Kumar, P. Nuhant, Y. Wang, J. L. Lauer, J. Liu, M. A. Istrate, T. M. Kamenecka, W. R. Roush, D. Vidović, et al. 2011. Suppression of TH17 differentiation and autoimmunity by a synthetic ROR ligand. *Nature* 472: 491–494.
59. Sundrud, M. S., S. B. Koralov, M. Feuerer, D. P. Calado, A. E. Kozhaya, A. Rhule-Smith, R. E. Lefebvre, D. Unutmaz, R. Mazitschek, H. Waldner, et al. 2009. Halofuginone inhibits TH17 cell differentiation by activating the amino acid starvation response. *Science* 324: 1334–1338.
60. Ishikawa, J., K. Ohga, T. Yoshino, R. Takezawa, A. Ichikawa, H. Kubota, and T. Yamada. 2003. A pyrazole derivative, YM-58483, potently inhibits store-operated sustained Ca2+ influx and IL-2 production in T lymphocytes. *J. Immunol.* 170: 4441–4449.
61. Zitt, C., B. Strauss, E. C. Schwarz, N. Spaeth, G. Rast, A. Hatzelmann, and M. Hoth. 2004. Potent inhibition of Ca2+ release-activated Ca2+ channels and T-lymphocyte activation by the pyrazole derivative BTP2. *J. Biol. Chem.* 279: 12427–12437.
62. Chen, G., S. Panicker, K. Y. Lau, S. Apparsundaram, V. A. Patel, S. L. Chen, R. Soto, J. K. Jung, P. Ravindran, D. Okuhara, et al. 2013. Characterization of a novel CRAC inhibitor that potently blocks human T cell activation and effector functions. *Mol. Immunol.* 54: 355–367.
63. Feske, S. 2009. ORAI1 and STIM1 deficiency in human and mice: roles of store-operated Ca2+ entry in the immune system and beyond. *Immunol. Rev.* 231: 189–209.